

1 An anti-Gn glycoprotein antibody from a convalescent patient potently
2 inhibits the infection of severe fever with thrombocytopenia syndrome virus

3

4 Ki Hyun Kim^{1,2}, Jinhee Kim³, Meehyun Ko³, June Young Chun⁴, Hyori Kim^{2,#a}, Seungtaek
5 Kim⁵, Ji-Young Min^{3,#b}, Wan Beom Park⁴, Myoung-don Oh⁴, and Junho Chung^{1,2,6,*}

6

7 ¹Department of Biochemistry and Molecular Biology, Seoul National University College of
8 Medicine, Seoul, Republic of Korea

9 ²Cancer Research Institute, Seoul National University College of Medicine, Seoul, Republic
10 of Korea

11 ³Respiratory Virus Laboratory, Institut Pasteur Korea, Gyeonggi-do, Republic of Korea.

12 ⁴Department of Internal Medicine, Seoul National University College of Medicine, Seoul,
13 Republic of Korea

14 ⁵Zoonotic Virus Laboratory, Institut Pasteur Korea, Gyeonggi-do, Republic of Korea.

15 ⁶Department of Biomedical Science, Seoul National University College of Medicine, Seoul,
16 Republic of Korea

17 ^{#a}Asan Institute for Life Sciences, Asan Medical Center, Seoul, Republic of Korea

18 ^{#b}Current affiliation: GlaxoSmithKline, Rockville, Maryland, United States of America

19

20 *Corresponding author

21 E-mail: jjhchung@snu.ac.kr (JC)

22 **Abstract**

23 Severe fever with thrombocytopenia syndrome (SFTS) is an emerging infectious
24 disease localized to China, Japan, and Korea that is characterized by severe hemorrhage and a
25 high fatality rate. Currently, no specific vaccine or treatment has been approved for this
26 disease. To develop a therapeutic agent for SFTS, we isolated antibodies from a phage-
27 displayed antibody library that was constructed from a patient who recovered from SFTS
28 virus (SFTSV) infection. One antibody, designated as Ab10, was reactive to the Gn envelope
29 glycoprotein of SFTSV and protected host cells and A129 mice from infection in both *in*
30 *vitro* and *in vivo* experiments. Notably, Ab10 protected 80% of mice, even when injected 5
31 days after inoculation with a lethal dose of SFTSV. Using cross-linker assisted mass
32 spectrometry and alanine scanning, we located the non-linear epitope of Ab10 on the Gn
33 glycoprotein domain II and an unstructured stem region, suggesting that Ab10 may inhibit a
34 conformational alteration that is critical for cell membrane fusion between the virus and host
35 cell. Ab10 reacted to recombinant Gn glycoprotein in Gangwon/Korea/2012, HB28, and SD4
36 strains. Additionally, based on its epitope, we predict that Ab10 binds the Gn glycoprotein in
37 247 of 272 reported SFTSV isolates previously reported. Together, these data suggest that
38 Ab10 has potential to be developed into a therapeutic agent that could protect against more
39 than 90% of reported SFTSV isolates.

40

41 **Author summary**

42 Severe fever with thrombocytopenia syndrome (SFTS) is an emerging infectious
43 disease localized to China, Japan, and Korea. This tick-borne virus has infected more than
44 5,000 humans with a 6.4% to 20.9% fatality rate. Currently, there are no prophylactic or
45 therapeutic measures against this virus. Historically, antibodies from patients who recovered

46 from viral infection have been used to treat new patients. Until now, one recombinant
47 monoclonal antibody was approved for the prophylaxis of respiratory syncytial virus infection.
48 We selected 10 antibodies from a patient who recovered from SFTS and found that one
49 antibody potentially inhibited SFTS viral infection in both test tube and animal studies. We
50 determined the binding site of this antibody to SFTS virus, which allowed us to predict that
51 this antibody could bind 247 out of 272 SFTS virus isolates reported up to now. We
52 anticipate that this antibody could be developed into a therapeutic measure against SFTS.

53

54 **Introduction**

55 Since its isolation as a novel virus in 2011, cases of the acute infectious disease called
56 severe fever with thrombocytopenia syndrome (SFTS)[1] have risen rapidly in China, Japan,
57 and Korea, posing a risk to public health and increasing the fear of ticks that transmit the
58 deadly SFTS virus (SFTSV). From 2011 to 2016, this emerging tick-borne virus infected
59 5,360 people in China with an average case fatality rate of 6.40%[2]. After initial reports in
60 2013 of sporadic SFTS cases in South Korea[3] and Japan[4], South Korea reported 605
61 cases with an average case fatality of 20.9%[5] and Japan reported 310 cases with an average
62 fatality of 19.4%[6] from 2013 to 2017.

63 Ticks such as *Haemaphysalis longicornis* and *Rhipicephalus microplus* are implicated as the
64 prominent vectors for transmitting SFTSV[7]. With regards to SFTSV hosts, various
65 vertebrate species are considered to have been infected, as evidenced by high SFTSV
66 seroprevalence in domestic animals in SFTS endemic regions[8,9]. Additionally, reported
67 cases of human-to-human transmission through contact with blood or body fluid, including
68 infections in healthcare workers from patients, pose a further threat to the public[10,11].
69 Furthermore, the discovery of *H. longicornis* tick in the United States indicates the possibility

70 that SFTSV could spread to other continents, highlighting the need to prevent disease
71 transmission[12].

72 SFTSV is a single-stranded negative-sense tripartite RNA virus that is classified as a member
73 of the *Phlebovirus* genus, *Phenuiviridae* family, and *Bunyaviriales* order. The genome of
74 SFTSV is comprised of L, M, and S segments, which encode RNA-dependent RNA
75 polymerase (L segment), envelope Gn glycoprotein (M segment), envelope Gc glycoprotein
76 (M segment), nucleoprotein, (S segment) and nonstructural proteins (S segment) [13]. A
77 phylogenetic analysis based on genome sequences of SFTSV isolates found substantial
78 genetic diversity and accumulated mutations, suggesting that SFTSV has existed for decades
79 at minimum[14,15]. However, the difference in virulence between these SFTSV sub-lineages
80 has yet to be determined.

81 The major clinical features of SFTS include high fever, fatigue, malaise, anorexia, nausea,
82 vomiting, diarrhea, thrombocytopenia, leukocytopenia, and abdominal pain[16,17]. In severe
83 cases, SFTS can include central nervous system manifestations, hemorrhagic signs, and
84 multiple organ dysfunction, which can lead to death[18-21]. No vaccines or therapeutics
85 specific for SFTS have been approved for human use. Recently, a Phase 3 clinical trial of
86 favipiravir (Avigan®), an drug approved for the treatment of influenza virus infection in
87 Japan, was initiated to expand its indication to SFTS treatment[22]. Monoclonal antibodies or
88 convalescent sera from SFTS patients were tested to identify potential therapeutic
89 intervention targets, resulting in the identification of SFTSV glycoproteins as molecules
90 required for host cell entry[23,24] and also as critical targets for virus neutralization through
91 the development of humoral immunity. However, generating an antibody for these targets in
92 infected humans was found to be rare, due to the presence of immunodominant decoy
93 epitopes in the nucleoprotein[25], which is a common phenomenon in a pathogenic virus-
94 infected host[26]. But in animal models, the protective effect of human convalescent sera was

95 shown, suggesting that antibody therapy is possible[27]. Thus far, MAb4-5 is the only human
96 neutralizing monoclonal antibody reported, and it was developed using a combinatorial
97 human antibody library from five patients[28]. MAb4-5 binds to domain III of SFTSV Gn
98 glycoprotein[29]. The neutralizing effect of MAb4-5 has been shown only in *in vitro*, and its
99 *in vivo* efficacy remains to be shown.

100 In this study, we constructed an antibody library from a patient who recovered from SFTS,
101 and selected antibodies against the Gn and Gc glycoproteins. Among these antibodies, Ab10
102 bound to Gn glycoprotein and showed a potent neutralizing effect both *in vitro* and *in vivo*. In
103 addition, we characterized the conformational epitope of Ab10 using crosslinking coupled
104 mass spectrometry and by testing its reactivity to alanine mutants, which allowed us to
105 estimate the strain coverage of Ab10.

106

107 **Results**

108 **Anti-Gn/Gc glycoprotein antibodies were selected from an antibody library generated** 109 **from a convalescent SFTS patient**

110 In human embryonic kidney (HEK) 293F cell, we produced Gn and Gc glycoproteins
111 fused with a crystallizable fragment of the human immunoglobulin (Ig) heavy chain constant
112 region (Gn-Fc and Gc-Fc) or those fused with the human Ig kappa light chain constant region
113 (Gn-C κ and Gc-C κ) and then purified the proteins. We constructed the phage-displayed
114 single-chain variable fragment (scFv) antibody library with a complexity of 1.3×10^9 using
115 peripheral blood mononuclear cells isolated from a patient who had recovered from SFTS.
116 The library was subjected to four rounds of biopanning against either the recombinant Gn-Fc
117 or the Gc-Fc fusion proteins conjugated to paramagnetic beads. We randomly selected
118 phagemid clones from the output titer plate from the last round of biopanning and subjected

119 these clones to phage enzyme-linked immunosorbent assay (ELISA). To minimize the
120 number of clones reactive to the Fc portion of fusion proteins, Gn-C κ and Gc-C κ were used
121 as antigens. Positive clones were selected and subjected to Sanger sequencing to determine
122 the scFv nucleotide sequence. We identified five clones reactive to Gn and five clones
123 reactive to Gc. All of these scFv clones were expressed as a scFv antibody fused with Fc
124 (scFv-Fc) in HEK293F cell and purified using affinity chromatography.

125

126 **Ab10 mAb potently inhibited the amplification of SFTSV *in vitro***

127 We tested 10 antibodies for their ability to reduce cytopathic effects (CPE) caused by
128 SFTSV (S1 Fig). One anti-Gn antibody, designated as Ab10, was extremely effective at
129 neutralizing SFTSV by reducing the percentage of cells showing CPE from 90% to 10%. The
130 V_H sequences of Ab10 had a 95.9% shared identity with the IGHV3-30*18 germline,
131 excluding the heavy chain complementary determining region (HCDR) 3, whereas the V _{κ}
132 sequence had 86.3% shared identity with the IGKV1-39*01 germline (S2 Fig).

133 In an immunofluorescence assay (IFA) using Vero cells and an anti-Gn antibody, we
134 determined the proportion of Gn glycoprotein producing cells, which were infected with
135 SFTSV, to measure the neutralizing potency of Ab10. Only $5.6 \pm 2.8\%$ (mean \pm s.d.) of Vero
136 cells produced Gn glycoprotein when Ab10 was treated at a concentration of 50 $\mu\text{g/ml}$ (956
137 nM) (Fig 1). Ab10 also showed a dose-dependent protective effect (S3 Fig). When MAb4-5
138 antibody was applied at the same concentration, $77.8 \pm 18.0\%$ of cells produced Gn
139 glycoprotein. When cells were not protected by any antibody, all cells produced Gn
140 glycoprotein and cells not incubated with SFTSV did not produce Gn glycoprotein.

141

142 **Ab10 protected mice from SFTSV infection, even with treatment delayed up to 3 days**

143 Type I interferon (interferon α/β) receptor gene (IFNAR1) deficient A129 mice (n = 5
144 per group) were subcutaneously injected with the Gangwon/Korea/2012 strain of SFTSV at a
145 dose of either 2 or 20 plaque forming units (PFU). After 1 h, mice were intraperitoneally
146 administered with either phosphate-buffered saline (PBS), Ab10, MAb4-5, or a human IgG₁
147 isotope control antibody at a dose of 600 μ g (approximately corresponding to 30 mg/kg of
148 body weight); for 4 days at 24 h intervals, the injection of the same amount of antibody was
149 performed (Fig 2A).

150 In the groups treated with PBS or an isotype control antibody, all mice died within 7
151 days at both viral doses (Fig 2B and 2C). At 4 days post infection (d.p.i.) with a dose of 2
152 PFU, approximately 10% of body weight was lost; at 3 d.p.i. with 20 PFU, 10–15% of body
153 weight was lost. All mice treated with Ab10 survived both viral doses and did not have any
154 weight loss. With MAb4-5 treatment, death occurred in all mice treated with a 2 PFU viral
155 dose and 80% of mice treated with a 20 PFU dose, and significant weight loss was observed
156 in all these mice.

157 In the delayed treatment model, the antibody treatment started from 1, 3, 4, or 5 d.p.i.
158 and continued for 4 consecutive days (Fig 3A). At a 2 PFU viral dose, all mice survived when
159 treatments with Ab10 were delayed until 3 d.p.i., and 80% survived when the treatment was
160 delayed until 4 d.p.i. or 5 d.p.i.(Fig 3B and 3C). Mice not treated until 4 d.p.i. had significant
161 weight loss. At a 20 PFU viral dose, delaying Ab10 antibody treatment until 1 or 3 d.p.i.
162 protected all or 80% of mice, respectively. Mice with treatment delayed until 1 d.p.i did not
163 lose weight, whereas mice with treatment delayed until 3 d.p.i. lost 8% of body weight. When
164 treatment was delayed until 4 d.p.i or later, all the mice died.

165

166 **Ab10 binds to recombinant Gn glycoprotein with high affinity in a broad variety of**
167 **strains**

168 To check the reactivity of Ab10 to SFTSV strains other than Gangwon/Korea/2012,
169 we overexpressed and purified recombinant Gn glycoproteins of other SFTSV strains.
170 Among the 272 SFTSV strain sequences deposited in the Virus Pathogen Database and
171 Analysis Resource (ViPR), we selected the strains HB29, AH15, SD4, YG1, which belong to
172 other clusters (S4 Fig), to compare their reactivity with well-known virus isolates from China
173 and Japan. We successfully overexpressed Gn glycoprotein from HB29 and SD4 as a Fc
174 fusion protein and subjected these proteins to ELISA. Ab10 IgG₁ successfully bound to Gn
175 glycoproteins from the HB29 and SD4 strains in a dose-dependent manner, at concentrations
176 ranging from 10 pM to 1 nM (Fig 4A). Further, the amount of antibody bound to the HB29
177 and SD4 Gn glycoproteins coated on the ELISA plate was higher than that of the
178 Gangwon/Korea/2012 glycoproteins, at most of the tested concentrations. We also found that
179 Mab4-5 was reactive to Gn glycoprotein from the HB29 and SD4 strains (Fig 4B).

180 We used surface plasmon resonance analysis to determine the kinetics of Ab10
181 binding to the Gn glycoprotein of Gangwon/Korea/2012. Ab10 bound to Gn glycoprotein
182 with an equilibrium dissociation constant (K_D) of 104 pM and found an association rate (K_{on})
183 of $7.4 \times 10^5 \text{ M}^{-1}\text{s}^{-1}$ and a dissociation rate (K_{off}) of $7.7 \times 10^{-5} \text{ s}^{-1}$ (Fig 4C).

184

185 **Ab10 binds to a non-linear epitope on domain II and the stem region of the Gn**
186 **glycoprotein**

187 In an immunoblot analysis using recombinant Gn glycoprotein from the
188 Gangwon/Korea/2012 strain, Ab10 did not react to Gn glycoprotein, whereas some other

189 anti-Gn antibodies were reactive (S5 Fig). Based on this observation, we concluded that the
190 antibody reacts to a non-linear epitope.

191 To discover the site where Ab10 binds, we performed crosslinking coupled mass
192 spectrometry using a deuterium isotope-labeled homo-bifunctional linker, which forms
193 covalent bonds between amino acid residues within the interface of the antibody-antigen
194 complex as described previously[30]. We found that cross-linkers bound to five amino acid
195 residues (318Y, 324R, 326K, 328Y, and 331S) within domain II of the SFTSV Gn
196 glycoprotein and also to four amino acid residues (371K, 372S, 379H, and 383S) within the
197 stem region (Fig 5A).

198 Based on this observation, we prepared several alanine-replacement mutants that
199 spanned from 315V to 389K and tested their reactivity to Ab10 using ELISA. All the mutants
200 were expressed with an HA peptide at the carboxy terminal and the tags were used to
201 measure the relative amount of each mutant. Alanine mutant proteins were captured by the
202 Ab10 antibody, which was coated on the ELISA plate. Then, we measured the amount of
203 captured mutant proteins by detecting the Fc portion of protein. The signals detected by
204 capturing the HA peptide were used to normalize expression of mutant proteins. We
205 measured the reactivity of Ab10 to alanine mutant Gn proteins, relative to wild type Gn
206 glycoprotein, and found that alanine replacement of the amino acid residues in domain II,
207 from V315 to M334, reduced the reactivity of Ab10 by more than 60%, except for S317,
208 G319, and M321. This finding was consistent with our results from the crosslinking coupled
209 mass spectrometry (Fig 5A and 5B).

210 In the stem region, replacing the cystine residues (C349, C356, C376, and C381)
211 reduced the relative reactivity by more than 80%. This observation was consistent with a
212 previous report that the structural stability of Gn was disrupted by a C356A mutation[29].
213 Also, mutation of the flanking residues of cystine, corresponding to G351, L354, E355, I357,

214 T374, and V375 also reduced the reactivity by over 60%. In the cases of mutation residues
215 which are distant from cysteine residues, mutation of G360, V361, R362, L363, T365, L370,
216 G387, and K389 residues reduced the relative reactivity by more than 80%. The other
217 residues had minor effects on reactivity. Overall, Ab10 binding to Gn was predicted to be
218 affected by 25 amino acid residues within domain II and the stem region of SFTSV Gn
219 glycoprotein. Because Gn glycoproteins from 247 isolates have conserved sequences for
220 these 25 amino acid residues, we expect that Ab10 can react with 90.8% (247 out of 272
221 isolates) of SFTSV isolates currently reported (S6 Fig).

222

223 **Discussion**

224 Antibodies play a pivotal role in preventing viral entry into cells and can kill infected
225 cells through antibody-dependent cellular cytotoxicity or complement-dependent
226 cytotoxicity[31-33]. Polysera from recovered patients or from vaccinated donors have been
227 used as prophylactic agents for various viral diseases, including hepatitis B and rabies[34].
228 As an alternative approach, monoclonal antibodies have also been developed and tested as
229 therapies or prophylaxis for viral diseases. Palivizumab (Synagis®) was market-approved for
230 the prophylaxis of respiratory syncytial virus (RSV) in 1998. Antibodies against HIV[35-37],
231 RSV[38], Ebola virus[39], and influenza virus[40,41] demonstrated potent efficacy in animal
232 models. Antibodies targeting emerging or re-emerging viruses, including MERS-CoV[42-44]
233 and Zika virus[45-47], were also developed and are being tested in clinical trials. In the past
234 several decades, antibodies have become the one of the major therapeutic agents for cancer
235 and autoimmune disease with indications that have rapidly broadened in recent years. The
236 recent technical improvements in the discovery and manufacturing steps of therapeutic

237 antibody production have also allowed rapid and successful antibody development to combat
238 emerging infectious diseases[48].

239 Until now, SFTS patients have been reported from China, South Korea, and Japan,
240 and the number of patients has increased each year[2,5,6]. However, SFTS fatality varies
241 among the three countries[21]. The average case fatality rate in China from 2011 to 2016 was
242 6.40%[2]. Those in South Korea and Japan after 2013 were much higher; 20.9%[5] or
243 19.4%[6], respectively. In the Virus Pathogen Database and Analysis Resource (ViPR), 272
244 sequences of SFTSV isolates are currently deposited. But it is unknown if there is any
245 significant variability in the virulence of these isolates. Previous reports showed that mice
246 died 5 to 7 days after infection with 10^6 focus forming units (FFU) of the YG1 strain[27] or
247 10^6 TCID₅₀ of the SPL010 strain[49]. Based on these observations, we first inoculated A129
248 mice with 2×10^5 PFU of the Gangwon/Korea/2012 strain and observed that all mice died 4
249 days after infection. With a 20 PFU dose of the Gangwon/Korea/2012 strain, mice died 5 to 7
250 days after infection.

251 We also observed that the amount of body weight losses at death were much higher in
252 our study than those in other studies.[49]. In our data, A129 mice died after losing 15% of
253 their body weight. But in the SPL010 strain, mice died after losing 30% of their body weight.
254 These results might be due to a difference in virulence between the strains. Differences in
255 virulence between strains of the Rift Valley fever virus (RVFV), a phlebovirus similar to
256 SFTSV, have been reported[50]. Or it might be due to differences in the animals tested,
257 because STAT2 knock out Syrian hamsters challenged with 10 PFU of the HB29 strain
258 showed a similar fatality rate[51].

259 The mechanisms of antibody inhibition of viral replication inside host cells have been
260 studied extensively, especially in the case of influenza virus. The most-widely known
261 mechanism is for an antibody to bind the portion of virus that interacts with the host cell

262 receptor, thereby blocking the interaction between the virus and the host cell[52]. Another
263 group of antibodies was reported to bind the stem region of influenza hemagglutinin that is
264 critical for conformational rearrangements that occur during membrane fusion[53-55]. This
265 mechanism has more potential to be utilized for clinical development, because the stem
266 region has fewer mutations than the receptor binding site. Additionally, several groups,
267 including ours, have elucidated unconventional virus neutralizing mechanisms that affect the
268 infection steps that occur after membrane fusion[56,57].

269 In our crosslinking coupled mass spectrometry and alanine mutant studies, the Ab10
270 epitope was confined to domain II and the stem region of the Gn glycoprotein. Although the
271 crystal structure of the phlebovirus Gn glycoprotein stem region has not yet been solved, a
272 recent report showed a cryo-electron microscopy map of RVFV, and depicted the crystal
273 structure of the RVFV Gn glycoprotein head region without a stem region[58]. The report
274 also describes the membrane fusion mechanism of RVFV that is mediated by a low pH
275 induced exposure of the hydrophobic Gc fusion loop. At a neutral pH, the Gn domain II (β -
276 ribbon domain) shields the Gc fusion loop in the pre-fusion state and prevents premature
277 fusion. Based on this report, we hypothesize that Ab10 simultaneously binds to domain II and
278 the stem region of the Gn glycoprotein and prevents un-shielding of the Gc fusion loop.

279 In conclusion, Ab10 is a monoclonal antibody that has shown therapeutic efficacy in a
280 mouse SFTSV infection model. Although the neutralization efficacy of Ab10 was only tested
281 in the Gangwon/Korea/2012 strain that was cultured in Vero cells, we confirmed its binding
282 capability to recombinant SFTSV Gn in the HB29 and SD4 strains, which are both from
283 China. According to the epitope revealed in this study, Ab10 is estimated to interact with the
284 majority of SFTSV isolates currently reported. Based on these results, we believe that Ab10
285 has sufficient potential to be developed as a prophylactic and therapeutic agent for a broad
286 variety of SFTS isolates.

287

288 **Materials and methods**

289 **Ethics statements: human subjects and animal models**

290 The studies involving recovered patient's blood samples were reviewed and approved
291 by the Institutional Ethics Review Board of Seoul National University Hospital (IRB
292 approval number: 1405-031-576). All of the patients were adults and submitted written
293 informed consent. All animal studies were conducted in an Animal Biosafety Level 3
294 (ABSL-3) facility at the Institut Pasteur Korea according to the principles established by the
295 Animal Protection Act and the Laboratory Animal Act in Republic of Korea. Interferon α/β
296 receptor knockout (IFNAR1^{-/-}, A129) mice (B&K Universal, Hull, UK) were bred, raised,
297 and genotyped at Institut Pasteur Korea. All experimental procedures were reviewed and
298 approved by the Institutional Animal Care and Use Committee at the Institut Pasteur Korea
299 (Animal protocol number: IPK-17003-1).

300

301 **Production of recombinant SFTSV Gn/Gc glycoprotein fusion proteins**

302 The SFTSV Gn glycoprotein amino acid sequences of various isolates used in this
303 study were retrieved from the Virus Pathogen Database and Analysis Resource (ViPR). To
304 obtain SFTSV Gn glycoprotein ectodomain coding DNA strands, human codon optimized
305 DNA sequences corresponding to amino acid sequences from 20 to 452 of GenBank
306 Accession No. ADZ04471 (Strain HB29), ADZ04477 (Strain SD4), ADZ04486 (Strain AH
307 15), BAN58185 (Strain YG1), AGT98506 (Strain Gangwon/Korea/2012) were synthesized
308 (GenScript, Piscataway, NJ, USA and Integrated DNA Technologies, Coralville, IA, USA).
309 Human codon optimized DNA sequence of SFTSV Gc ectodomain of strain
310 Gangwon/Korea/2012, corresponding to the sequence from 563 to 1035 of AGT98506, was

311 also synthesized. For the overexpression and purification of recombinant SFTSV Gn / Gc
312 glycoprotein ectodomain fused to the Fc region of human immunoglobulin heavy constant
313 gamma1 (IGHG1), termed Gn-Fc / Gc-Fc, or fused to the human immunoglobulin kappa
314 constant region (IGKC), termed Gn-C κ / Gn-C κ , SFTSV Gn / Gc glycoprotein ectodomain
315 encoding genes were cloned into the modified pCEP4 vector (V04450, Invitrogen, Carlsbad,
316 CA, USA) with a leader sequence of the human immunoglobulin kappa chain, two *Sfi*I
317 restriction enzyme sites, and the Fc region of human IGHG1 or human immunoglobulin
318 kappa constant region, as previously described[59,60]. Subsequently, the vectors were used
319 to transfect HEK 293F (R79007, Invitrogen) or Expi293F cells (A14527, Invitrogen) using
320 polyethylenimine (23966-1, Polysciences, Warrington, PA, USA), then the transfected cells
321 were cultured in FreeStyle™ 293 expression medium (12338026, Gibco, Thermo Fisher
322 Scientific, Waltham, MA, USA). Overexpressed recombinant SFTSV Gn and Gc
323 glycoprotein fusion proteins were purified by affinity chromatography using MabSelect™ or
324 KappaSelect™ columns with the ÄKTA Pure chromatography system (11003495, 17545811,
325 29018225, GE Healthcare, Chicago, IL, USA), following the protocol provided by the
326 manufacturer.

327 For alanine-scanning mutagenesis, SFTSV Gn glycoprotein with amino acid residues (315-
328 389) substituted with alanine were produced by cloning synthesized DNA fragments
329 (Integrated DNA Technologies) into modified pCEP4 vector, as described above.

330 Subsequently, influenza hemagglutinin (HA) tag sequence (YPYDVPDYA) was introduced
331 to the C-terminus of the Fc region of human immunoglobulin heavy gamma1 and the whole
332 protein, designated as Gn-Fc-HA, was produced as described above.

333 In order to produce histidine tagged SFTSV Gn glycoprotein, a ligand for surface plasmon
334 resonance analysis, a Gn-C κ with six carboxy-terminal poly-histidine residues was designed
335 and produced as described above.

336

337 **Human antibody library construction and antibody selection**

338 Peripheral blood mononuclear cells of a patient who recovered from SFTS were
339 collected using a Ficoll-Paque density gradient medium (17144002, GE Healthcare). Total
340 RNA was isolated using TRIzol Reagent (15596018, Invitrogen), and cDNA was synthesized
341 using a SuperScript III first-strand cDNA synthesis kit with oligo dT priming (18080051,
342 Invitrogen). From this cDNA, a phage-display library of human single-chain variable
343 fragments (scFv) was constructed, and four rounds of biopanning were performed to select
344 scFv antibody clones from the library, as previously described[61,62]. For each round of
345 biopanning, recombinant SFTSV Gn-Fc coated onto paramagnetic Dynabeads (14302D,
346 Invitrogen) were used. To select SFTSV glycoprotein binding clones, phage ELISA was
347 performed as previously described, using Gn or Gc glycoprotein -coated microtiter plates,
348 scFv displaying phages, and horseradish peroxidase (HRP) conjugated anti-M13 antibody
349 (11973-MM05, Sino Biological, Beijing, China)[62]. The nucleotide sequences of positive
350 scFv clones were determined by Sanger nucleotide sequencing (Cosmogenetech, South
351 Korea). Germline sequences of selected antibody variable regions were analyzed by the
352 National Center for Biotechnology Information (NCBI) IgBLAST.

353

354 **Production of single-chain variable fragment antibodies and IgG₁ antibodies against** 355 **SFTSV Gn glycoprotein**

356 The genes encoding the variable heavy chain and variable light chain of Ab10 and
357 MAb4-5[28] were synthesized (Integrated DNA Technologies, GenScript) and fused with
358 human heavy chain constant region gene (IgG₁) and human kappa light chain gene, and then
359 cloned into an eukaryotic expression vector, as described previously[63,64]. The expression

360 vectors were transfected into HEK 293F cells. The IgG₁ molecule was purified from the
361 culture supernatant by affinity chromatography using MabSelect™ as described above.
362 Genes encoding the scFv-Fc fusion protein and the scFv-Cκ fusion protein were synthesized
363 and cloned into a pCEP4 vector (Invitrogen). After transfection into HEK 293F cells, the
364 recombinant proteins were overexpressed and purified as described above.

365

366 **SFTSV preparation and immunofluorescent imaging-based neutralization test**

367 The SFTSV strain of Gangwon/Korea/2012[3] was propagated in Vero cells (10081,
368 Korean Cell Link Bank) with Roswell Park Memorial Institute (RPMI)-1640 medium (LM
369 011-01, Welgene, Daegu, South Korea) supplemented with 2% heat-inactivated fetal bovine
370 serum (16000044, Gibco) and penicillin-streptomycin (10378016, Gibco). The fifty-percent
371 tissue culture infective dose (TCID₅₀) values were titrated on Vero cells using the Reed-
372 Muench method[65]. Ab10 or MAB4-5 scFv-Fc fusion protein was serially diluted in 10-fold
373 increments from a 50 µg/ml concentration, then mixed with an equal volume of 100 TCID₅₀
374 SFTSV, and incubated at 37°C for 1 h. The virus-antibody mixture was transferred onto Vero
375 cells in 8-well chamber slides (154534, Thermo Scientific, Waltham, MA, USA) and
376 incubated at 37°C for 1 h. For the no infection control group, no virus was added to cells. In
377 contrast, for the infection control group, no antibody was incubated with virus. After
378 removing the virus-antibody mixture, cells were cultured for 2 days. For the IFA, cultured
379 cells were fixed with 4% paraformaldehyde in PBS for 1 h at room temperature. Slides were
380 blocked and permeabilized with PBS containing 0.1% Triton X-100 and 1% bovine serum
381 albumin, followed by incubation with 5 µg/ml of anti-SFTSV Gn glycoprotein antibody[66]
382 at 4°C overnight. After washing, cells were incubated for 1 h at room temperature with 1:100
383 diluted fluorescein isothiocyanate (FITC)-conjugated anti-rabbit IgG Fc antibody (111-095-
384 046, Jackson ImmunoResearch, West Grove, PA, USA). To stain the nucleus, 4',6-

385 Diamidino-2-phenylindole dihydrochloride (DAPI) was used. Fluorescence image of cells
386 was monitored under a confocal laser scanning microscope (TCS SP8, Leica, Wetzlar,
387 Germany).

388

389 ***In vivo* efficacy test**

390 For animal experiments, the titer of SFTSV was measured by plaque forming
391 assay[67]. Either 2 or 20 plaque forming units (PFU) of Gangwon/Korea/2012 strain SFTSV
392 in 200 µl of PBS were inoculated in 8- to 10-week-old male or female A129 mice by a
393 subcutaneous (s.c.) injection route. After an hour of infection, mice were administered with
394 Ab10 IgG₁ antibody or a PBS vehicle control through an intraperitoneal (i.p.) injection route,
395 at 30 mg/kg of body weight for every 24 h for a consecutive 4 days. Palivizumab
396 (MedImmune, Gaithersburg, MD, USA) or Mab4-5 IgG₁ was used as an isotype control or a
397 positive control antibody, respectively. In the delayed treatment model, the infected mice
398 were treated with antibodies at 1, 3, 4, or 5 days post infection (d.p.i.) for 4 days
399 consecutively. Body weight and survival of mice were monitored until 10 days post infection.

400

401 **Enzyme-linked immunosorbent assays**

402 In order to measure the binding activities of the Ab10 and MAb4-5 IgG₁ antibodies,
403 96-well half-area microplates (3690, Corning, Corning, NY, USA) were coated with Gn-Fc
404 fusion protein and incubated at 4°C overnight. Plates were blocked with 3% skim milk in
405 PBS for 1 h at room temperature. The plates were then washed with PBS and received
406 antibodies that were 10-fold serially diluted from 1 µM to 10 µM in blocking buffer. The
407 plates were then incubated for 2 h at room temperature and washed three times with 0.05%
408 Tween20 in PBS solution. Then, 50 µl of HRP-conjugated anti-human Ig kappa light chain
409 antibody (AP502P, Chemicon, Temecula, CA, USA) diluted in blocking buffer (1:5000) was

410 added into each well. Then, plates were incubated for 1 h at room temperature. After
411 washing, each well received 50 μ l of 3,3',5,5'-Tetramethylbenzidine (TMB) substrate
412 solution (34028, Thermo Scientific). The coloring reaction was stopped by adding 50 μ l of 2
413 M sulfuric acid. The absorbance of each well was measured at 450 nm using a microplate
414 spectrophotometer (Multiskan GO, Thermo Scientific).

415

416 **Surface plasmon resonance analysis of Ab10**

417 The kinetics of Ab10 and Gn glycoprotein binding were measured by surface plasmon
418 resonance analysis, using a Biacore T200 instrument with sensor chip CM5, amine coupling
419 kit, and his capture kit (28975001, 29149603, BR100050, 28995056, GE Healthcare). We
420 followed the recommended manufacturer's protocol for the procedures and conditions of
421 reaction buffers, flow times, flow rates, and concentration of analytes. Briefly, anti-histidine
422 antibody was immobilized on an activated CM5 chip, followed by a deactivation step. Then,
423 histidine tagged Gn-Ck was injected over the flow cells prior to antibody injection. For the
424 association step, all of the Ab10 IgG₁ antibody in PBS at concentrations of two-fold
425 increments ranging from 1.25 nM to 80 nM was injected for 3 min. For the dissociation step,
426 PBS containing 0.005% of Tween20 was injected for 5 min. After each dissociation step,
427 chip regeneration was performed.

428

429 **Conformational epitope mapping by crosslinking coupled mass spectrometry**

430 The epitope of Ab10 antibody was first determined by analyzing the complex of Ab10
431 antibody and SFTSV Gn-Ck antigen linked with deuterated cross-linkers, as previously
432 described[30]. Briefly, antibody, antigen, and antibody/antigen complex were characterized
433 by the high mass matrix-assisted laser desorption/ionization (MALDI) mass spectrometry

434 using a MALDI ToF/ToF tandem mass spectrometer (Autoflex III, Bruker, Billerica, MA,
435 USA) equipped with an interaction module (HM4, CovalX, Zürich, Switzerland). Afterwards,
436 the antibody/antigen complex was crosslinked with DSS d0/d12 isotope-labeled
437 homobifunctional N-hydroxysuccinimide esters, followed by reduction alkylation using
438 dithiothreitol, iodoacetamide, and urea. To digest the reduced complex, a proteolytic buffer
439 composed of trypsin, chymotrypsin, endoproteinase Asp-N, elastase, and thermolysin was
440 used. The sample was then analyzed by nano-liquid chromatography (Ultimate 3000, Dionex,
441 Sunnyvale, CA, USA) and Orbitrap mass spectrometry (Q Exactive Hybrid Quadrupole-
442 Orbitrap, Thermo Scientific).

443

444 **ELISA for epitope mapping**

445 To measure the binding activities of Ab10 to mutated Gn, Ab10 scFv-C κ antibody
446 and an anti-influenza virus hemagglutinin antibody (clone 12CA5, Bio X Cell, Lebanon, NH,
447 USA) were coated on a microplate in parallel. Then, plates were blocked with 3% skim milk
448 in PBS for 1 h at room temperature. Transiently transfected supernatant containing
449 recombinant Gn-Fc-HA proteins with alanine substitution was added to each well. After
450 incubation for 2 h at room temperature, the microplate was washed three times with 0.05%
451 Tween20 in PBS solution. Then, HRP-conjugated anti-human IgG Fc antibody (31423,
452 Invitrogen) diluted in blocking buffer was added to each well. The plate was incubated for 1
453 h at room temperature. After washing, each well received 50 μ l of 3,3',5,5'-
454 Tetramethylbenzidine (TMB) substrate solution (34028, Thermo Scientific). The coloring
455 reaction was stopped by adding 50 μ l of 2 M sulfuric acid. The absorbance of each well was
456 measured at 450 nm using a microplate spectrophotometer (Multiskan GO, Thermo
457 Scientific). Relative reactivity was calculated using absorbance values (Abs) as follows: %
458 Relative reactivity = [100 x {(Abs of mutant captured by Ab10) / (Abs of mutant captured by

459 HA antibody)} / {(Abs of wildtype captured by Ab10) / (Abs of wildtype captured by HA
460 antibody)}}].

461

462 **Data analysis**

463 ELISA and IFA data, including statistical comparisons, were analyzed and graphed
464 using GraphPad Prism software. Fluorescent signal measured by confocal microscope was
465 quantified using Leica Application Suite Advanced Fluorescence software. Mass
466 spectrometry data were analyzed using XQuest and Stavrox software. Plasmon surface
467 resonance data were analyzed using BIAevaluation software. Visualization, alignment, and
468 phylogenetic analysis of amino acid sequences were performed with Geneious software.

469

470 **Acknowledgements**

471 We thank Myung Jin Lee and Su Jin Choi for setting up the initial experimental conditions
472 for the virus neutralization assay.

473

474 **References**

- 475 1. Yu X-J, Liang M-F, Zhang S-Y, Liu Y, Li J-D, Sun Y-L, et al. Fever with
476 Thrombocytopenia Associated with a Novel Bunyavirus in China. *N Engl J Med.*
477 2011;364: 1523–1532. doi:10.1056/NEJMoa1010095
- 478 2. Sun J, Lu L, Wu H, Yang J, Ren J, Liu Q. The changing epidemiological
479 characteristics of severe fever with thrombocytopenia syndrome in China, 2011-2016.
480 *Sci Rep.* 2017;7: 9236. doi:10.1038/s41598-017-08042-6
- 481 3. Kim K-H, Yi J, Kim G, Choi SJ, Jun KI, Kim N-H, et al. Severe fever with
482 thrombocytopenia syndrome, South Korea, 2012. *Emerging Infect Dis.* 2013;19:
483 1892–1894. doi:10.3201/eid1911.130792
- 484 4. Takahashi T, Maeda K, Suzuki T, Ishido A, Shigeoka T, Tominaga T, et al. The first
485 identification and retrospective study of Severe Fever with Thrombocytopenia

- 486 Syndrome in Japan. *J Infect Dis*. Oxford University Press; 2014;209: 816–827.
487 doi:10.1093/infdis/jit603
- 488 5. Korea Centers for Disease Control and Prevention. Disease information (Severe Fever
489 with Thrombocytopenia Syndrome, SFTS). In: *cdc.go.kr* [Internet]. 9 Feb 2018 [cited
490 22 Jun 2018]. Available:
491 [http://www.cdc.go.kr/CDC/health/CdcKrHealth0101.jsp?menuIds=HOME001-](http://www.cdc.go.kr/CDC/health/CdcKrHealth0101.jsp?menuIds=HOME001-MNU1132-MNU1147-MNU0746-MNU2423&fid=7956&cid=70361)
492 [MNU1132-MNU1147-MNU0746-MNU2423&fid=7956&cid=70361](http://www.cdc.go.kr/CDC/health/CdcKrHealth0101.jsp?menuIds=HOME001-MNU1132-MNU1147-MNU0746-MNU2423&fid=7956&cid=70361)
- 493 6. National Institute of Infectious Diseases, Japan. Severe Fever with Thrombocytopenia
494 Syndrome (SFTS). In: *niid.go.jp* [Internet]. 25 Jul 2018 [cited 15 Aug 2018].
495 Available: <https://www.niid.go.jp/niid/ja/diseases/sa/sfts.html>
- 496 7. Zhang Y-Z, Zhou D-J, Qin X-C, Tian J-H, Xiong Y, Wang J-B, et al. The ecology,
497 genetic diversity, and phylogeny of Huaiyangshan virus in China. *Journal of Virology*.
498 *American Society for Microbiology*; 2012;86: 2864–2868. doi:10.1128/JVI.06192-11
- 499 8. Niu G, Li J, Liang M, Jiang X, Jiang M, Yin H, et al. Severe fever with
500 thrombocytopenia syndrome virus among domesticated animals, China. *Emerging*
501 *Infect Dis*. 2013;19: 756–763. doi:10.3201/eid1905.120245
- 502 9. Zhang Y-Z, Xu J. The emergence and cross species transmission of newly discovered
503 tick-borne Bunyavirus in China. *Current Opinion in Virology*. 2016;16: 126–131.
504 doi:10.1016/j.coviro.2016.02.006
- 505 10. Liu Y, Li Q, Hu W, Wu J, Wang Y, Mei L, et al. Person-to-person transmission of
506 severe fever with thrombocytopenia syndrome virus. *Vector Borne Zoonotic Dis*.
507 2012;12: 156–160. doi:10.1089/vbz.2011.0758
- 508 11. Gai Z, Liang M, Zhang Y, Zhang S, Jin C, Wang S-W, et al. Person-to-Person
509 Transmission of Severe Fever With Thrombocytopenia Syndrome Bunyavirus
510 Through Blood Contact. *Clin Infect Dis*. Oxford University Press; 2012;54: 249–252.
511 doi:10.1093/cid/cir776
- 512 12. Rainey T, Occi JL, Robbins RG, Egizi A. Discovery of *Haemaphysalis longicornis*
513 (Ixodida: Ixodidae) Parasitizing a Sheep in New Jersey, United States. *J Med Entomol*.
514 Oxford University Press; 2018;55: 757–759. doi:10.1093/jme/tjy006
- 515 13. Liu S, Chai C, Wang C, Amer S, Lv H, He H, et al. Systematic review of severe fever
516 with thrombocytopenia syndrome: virology, epidemiology, and clinical characteristics.
517 *Rev Med Virol*. Wiley-Blackwell; 2014;24: 90–102. doi:10.1002/rmv.1776
- 518 14. Liu L, Chen W, Yang Y, Jiang Y. Molecular evolution of fever, thrombocytopenia and
519 leukocytopenia virus (FTLSV) based on whole-genome sequences. *Infection, Genetics*
520 *and Evolution*. 2016;39: 55–63.
- 521 15. Zhan J, Wang Q, Cheng J, Hu B, Li J, Zhan F, et al. Current status of severe fever with
522 thrombocytopenia syndrome in China. *Virologica Sinica*. Springer Singapore;
523 2017;32: 51–62. doi:10.1007/s12250-016-3931-1

- 524 16. Liu Q, He B, Huang S-Y, Wei F, Zhu X-Q. Severe fever with thrombocytopenia
525 syndrome, an emerging tick-borne zoonosis. *Lancet Infect Dis.* 2014;14: 763–772.
526 doi:10.1016/S1473-3099(14)70718-2
- 527 17. Kato H, Yamagishi T, Shimada T, Matsui T, Shimojima M, Saijo M, et al.
528 Epidemiological and Clinical Features of Severe Fever with Thrombocytopenia
529 Syndrome in Japan, 2013–2014. Xing Z, editor. *PLoS ONE*. Public Library of Science;
530 2016;11: e0165207. doi:10.1371/journal.pone.0165207
- 531 18. Gai Z-T, Zhang Y, Liang M-F, Jin C, Zhang S, Zhu C-B, et al. Clinical Progress and
532 Risk Factors for Death in Severe Fever with Thrombocytopenia Syndrome Patients. *J*
533 *Infect Dis.* Oxford University Press; 2012;206: 1095–1102. doi:10.1093/infdis/jis472
- 534 19. Ding Y-P, Liang MF, Ye J-B, Liu Q-H, Xiong C-H, Long B, et al. Prognostic value of
535 clinical and immunological markers in acute phase of SFTS virus infection. *Clin*
536 *Microbiol Infect.* 2014;20: O870–8. doi:10.1111/1469-0691.12636
- 537 20. Shin J, Kwon D, Youn S-K, Park J-H. Characteristics and Factors Associated with
538 Death among Patients Hospitalized for Severe Fever with Thrombocytopenia
539 Syndrome, South Korea, 2013. *Emerging Infect Dis.* 2015;21: 1704–1710.
540 doi:10.3201/eid2110.141928
- 541 21. Li H, Lu Q-B, Xing B, Zhang S-F, Liu K, Du J, et al. Epidemiological and clinical
542 features of laboratory-diagnosed severe fever with thrombocytopenia syndrome in
543 China, 2011–17: a prospective observational study. *Lancet Infect Dis.* Elsevier; 2018.
544 doi:10.1016/S1473-3099(18)30293-7
- 545 22. Cyranoski D. East Asia braces for surge in deadly tick-borne virus. *Nature.* 2018;556:
546 282–283. doi:10.1038/d41586-018-04486-6
- 547 23. Hofmann H, Li X, Zhang X, Liu W, Kühl A, Kaup F, et al. Severe fever with
548 thrombocytopenia virus glycoproteins are targeted by neutralizing antibodies and can
549 use DC-SIGN as a receptor for pH-dependent entry into human and animal cell lines.
550 *Journal of Virology.* American Society for Microbiology; 2013;87: 4384–4394.
551 doi:10.1128/JVI.02628-12
- 552 24. Sun Y, Qi Y, Liu C, Gao W, Chen P, Fu L, et al. Nonmuscle myosin heavy chain IIA
553 is a critical factor contributing to the efficiency of early infection of severe fever with
554 thrombocytopenia syndrome virus. *Journal of Virology.* American Society for
555 Microbiology; 2014;88: 237–248. doi:10.1128/JVI.02141-13
- 556 25. Yu L, Zhang L, Sun L, Lu J, Wu W, Li C, et al. Critical Epitopes in the Nucleocapsid
557 Protein of SFTS Virus Recognized by a Panel of SFTS Patients Derived Human
558 Monoclonal Antibodies. Dübel S, editor. *PLoS ONE*. Public Library of Science;
559 2012;7: e38291. doi:10.1371/journal.pone.0038291
- 560 26. Jin J, Park C, Cho S-H, Chung J. The level of decoy epitope in PCV2 vaccine affects
561 the neutralizing activity of sera in the immunized animals. *Biochemical and*
562 *Biophysical Research Communications.* 2018;496: 846–851.
563 doi:10.1016/j.bbrc.2018.01.141

- 564 27. Shimada S, Posadas-Herrera G, Aoki K, Morita K, Hayasaka D. Therapeutic effect of
565 post-exposure treatment with antiserum on severe fever with thrombocytopenia
566 syndrome (SFTS) in a mouse model of SFTS virus infection. *Virology*. 2015;482: 19–
567 27. doi:10.1016/j.virol.2015.03.010
- 568 28. Guo X, Zhang L, Zhang W, Chi Y, Zeng X, Li X, et al. Human antibody neutralizes
569 severe Fever with thrombocytopenia syndrome virus, an emerging hemorrhagic Fever
570 virus. *Clin Vaccine Immunol*. American Society for Microbiology; 2013;20: 1426–
571 1432. doi:10.1128/CVI.00222-13
- 572 29. Wu Y, Zhu Y, Gao F, Jiao Y, Oladejo BO, Chai Y, et al. Structures of phlebovirus
573 glycoprotein Gn and identification of a neutralizing antibody epitope. *Proc Natl Acad
574 Sci USA*. National Acad Sciences; 2017;114: E7564–E7573.
575 doi:10.1073/pnas.1705176114
- 576 30. Pimenova T, Nazabal A, Roschitzki B, Seebacher J, Rinner O, Zenobi R. Epitope
577 mapping on bovine prion protein using chemical cross-linking and mass spectrometry.
578 *Journal of Mass Spectrometry*. Wiley-Blackwell; 2008;43: 185–195.
579 doi:10.1002/jms.1280
- 580 31. Corti D, Misasi J, Mulangu S, Stanley DA, Kanekiyo M, Wollen S, et al. Protective
581 monotherapy against lethal Ebola virus infection by a potently neutralizing antibody.
582 *Science*. American Association for the Advancement of Science; 2016;351: 1339–
583 1342. doi:10.1126/science.aad5224
- 584 32. Liu Q, Fan C, Li Q, Zhou S, Huang W, Wang L, et al. Antibody-dependent-cellular-
585 cytotoxicity-inducing antibodies significantly affect the post-exposure treatment of
586 Ebola virus infection. *Sci Rep*. Nature Publishing Group; 2017;7: 45552.
587 doi:10.1038/srep45552
- 588 33. Gunn BM, Yu W-H, Karim MM, Brannan JM, Herbert AS, Wec AZ, et al. A Role for
589 Fc Function in Therapeutic Monoclonal Antibody-Mediated Protection against Ebola
590 Virus. *Cell Host & Microbe*. Elsevier; 2018;24: 221–233.e5.
591 doi:10.1016/j.chom.2018.07.009
- 592 34. Walker LM, Burton DR. Passive immunotherapy of viral infections: “super-
593 antibodies” enter the fray. *Nat Rev Immunol*. Nature Publishing Group; 2018;18: 297–
594 308. doi:10.1038/nri.2017.148
- 595 35. Bar KJ, Sneller MC, Harrison LJ, Justement JS, Overton ET, Petrone ME, et al. Effect
596 of HIV Antibody VRC01 on Viral Rebound after Treatment Interruption. *N Engl J
597 Med*. 2016;375: 2037–2050. doi:10.1056/NEJMoa1608243
- 598 36. Scheid JF, Horwitz JA, Bar-On Y, Kreider EF, Lu C-L, Lorenzi JCC, et al. HIV-1
599 antibody 3BNC117 suppresses viral rebound in humans during treatment interruption.
600 *Nature*. 2016;535: 556–560. doi:10.1038/nature18929
- 601 37. Caskey M, Schoofs T, Gruell H, Settler A, Karagounis T, Kreider EF, et al. Antibody
602 10-1074 suppresses viremia in HIV-1-infected individuals. *Nat Med*. Nature
603 Publishing Group; 2017;23: 185–191. doi:10.1038/nm.4268

- 604 38. Zhu Q, McLellan JS, Kallewaard NL, Ulbrandt ND, Palaszynski S, Zhang J, et al. A
605 highly potent extended half-life antibody as a potential RSV vaccine surrogate for all
606 infants. *Sci Transl Med. American Association for the Advancement of Science*;
607 2017;9: eaaj1928. doi:10.1126/scitranslmed.aaj1928
- 608 39. PREVAIL II Writing Group, Multi-National PREVAIL II Study Team, Davey RT,
609 Dodd L, Proschan MA, Neaton J, et al. A Randomized, Controlled Trial of ZMapp for
610 Ebola Virus Infection. *N Engl J Med. Massachusetts Medical Society*; 2016;375:
611 1448–1456. doi:10.1056/NEJMoa1604330
- 612 40. Yu F, Song H, Wu Y, Chang SY, Wang L, Li W, et al. A Potent Germline-like Human
613 Monoclonal Antibody Targets a pH-Sensitive Epitope on H7N9 Influenza
614 Hemagglutinin. *Cell Host & Microbe. Cell Press*; 2017;22: 471–483.e5.
615 doi:10.1016/j.chom.2017.08.011
- 616 41. Paules CI, Lakdawala S, McAuliffe JM, Paskel M, Vogel L, Kallewaard NL, et al. The
617 Hemagglutinin A Stem Antibody MEDI8852 Prevents and Controls Disease and
618 Limits Transmission of Pandemic Influenza Viruses. *J Infect Dis. 8 ed. 2017*;216:
619 356–365. doi:10.1093/infdis/jix292
- 620 42. Ying T, Du L, Ju TW, Prabakaran P, Lau CCY, Lu L, et al. Exceptionally potent
621 neutralization of Middle East respiratory syndrome coronavirus by human monoclonal
622 antibodies. Doms RW, editor. *Journal of Virology. American Society for*
623 *Microbiology*; 2014;88: 7796–7805. doi:10.1128/JVI.00912-14
- 624 43. Corti D, Zhao J, Pedotti M, Simonelli L, Agnihothram S, Fett C, et al. Prophylactic
625 and postexposure efficacy of a potent human monoclonal antibody against MERS
626 coronavirus. *PNAS. National Academy of Sciences*; 2015;112: 10473–10478.
627 doi:10.1073/pnas.1510199112
- 628 44. Pascal KE, Coleman CM, Mujica AO, Kamat V, Badithe A, Fairhurst J, et al. Pre- and
629 postexposure efficacy of fully human antibodies against Spike protein in a novel
630 humanized mouse model of MERS-CoV infection. *PNAS. National Academy of*
631 *Sciences*; 2015;112: 8738–8743. doi:10.1073/pnas.1510830112
- 632 45. Sapparapu G, Fernandez E, Kose N, Bin Cao, Fox JM, Bombardi RG, et al.
633 Neutralizing human antibodies prevent Zika virus replication and fetal disease in mice.
634 *Nature. 2016*;540: 443–447. doi:10.1038/nature20564
- 635 46. Wang Q, Yang H, Liu X, Dai L, Ma T, Qi J, et al. Molecular determinants of human
636 neutralizing antibodies isolated from a patient infected with Zika virus. *Sci Transl*
637 *Med. American Association for the Advancement of Science*; 2016;8: 369ra179–
638 369ra179. doi:10.1126/scitranslmed.aai8336
- 639 47. Robbiani DF, Bozzacco L, Keeffe JR, Khouri R, Olsen PC, Gazumyan A, et al.
640 Recurrent Potent Human Neutralizing Antibodies to Zika Virus in Brazil and Mexico.
641 *Cell. 2017*;169: 597–609.e11. doi:10.1016/j.cell.2017.04.024

- 642 48. Marston HD, Paules CI, Fauci AS. Monoclonal Antibodies for Emerging Infectious
643 Diseases - Borrowing from History. *N Engl J Med.* 2018;378: 1469–1472.
644 doi:10.1056/NEJMp1802256
- 645 49. Tani H, Fukuma A, Fukushi S, Taniguchi S, Yoshikawa T, Iwata-Yoshikawa N, et al.
646 Efficacy of T-705 (Favipiravir) in the Treatment of Infections with Lethal Severe
647 Fever with Thrombocytopenia Syndrome Virus. Duprex WP, editor. *mSphere.* 2016;1:
648 e00061–15. doi:10.1128/mSphere.00061-15
- 649 50. Ikegami T, Balogh A, Nishiyama S, Lokugamage N, Saito TB, Morrill JC, et al.
650 Distinct virulence of Rift Valley fever phlebovirus strains from different genetic
651 lineages in a mouse model. McElroy AK, editor. *PLoS ONE. Public Library of*
652 *Science;* 2017;12: e0189250. doi:10.1371/journal.pone.0189250
- 653 51. Gowen BB, Westover JB, Miao J, Van Wettere AJ, Rigas JD, Hickerson BT, et al.
654 Modeling Severe Fever with Thrombocytopenia Syndrome Virus Infection in Golden
655 Syrian Hamsters: Importance of STAT2 in Preventing Disease and Effective
656 Treatment with Favipiravir. Ross SR, editor. *Journal of Virology. American Society*
657 *for Microbiology;* 2017;91: e01942–16. doi:10.1128/JVI.01942-16
- 658 52. Weis W, Brown JH, Cusack S, Paulson JC, Skehel JJ, Wiley DC. Structure of the
659 influenza virus haemagglutinin complexed with its receptor, sialic acid. *Nature.*
660 1988;333: 426–431. doi:10.1038/333426a0
- 661 53. Tharakaraman K, Subramanian V, Cain D, Sasisekharan V, Sasisekharan R. Broadly
662 Neutralizing Influenza Hemagglutinin Stem-Specific Antibody CR8020 Targets
663 Residues that Are Prone to Escape due to Host Selection Pressure. *Cell Host &*
664 *Microbe.* Elsevier; 2014;15: 644–651. doi:10.1016/j.chom.2014.04.009
- 665 54. Wu Y, Cho M, Shore D, Song M, Choi J, Jiang T, et al. A potent broad-spectrum
666 protective human monoclonal antibody crosslinking two haemagglutinin monomers of
667 influenza A virus. *Nat Comms. Nature Publishing Group;* 2015;6: 7708.
668 doi:10.1038/ncomms8708
- 669 55. Chai N, Swem LR, Park S, Nakamura G, Chiang N, Estevez A, et al. A broadly
670 protective therapeutic antibody against influenza B virus with two mechanisms of
671 action. *Nat Comms. Nature Publishing Group;* 2017;8: 14234.
672 doi:10.1038/ncomms14234
- 673 56. VanBlargan LA, Goo L, Pierson TC. Deconstructing the Antiviral Neutralizing-
674 Antibody Response: Implications for Vaccine Development and Immunity.
675 *Microbiology and Molecular Biology Reviews. American Society for Microbiology;*
676 2016;80: 989–1010. doi:10.1128/MMBR.00024-15
- 677 57. Yoon A, Yi KS, Chang SY, Kim SH, Song M, Choi JA, et al. An Anti-Influenza Virus
678 Antibody Inhibits Viral Infection by Reducing Nucleus Entry of Influenza
679 Nucleoprotein. *PLoS ONE.* 2015;10: e0141312. doi:10.1371/journal.pone.0141312

- 680 58. Halldorsson S, Li S, Li M, Harlos K, Bowden TA, Huiskonen JT. Shielding and
681 activation of a viral membrane fusion protein. *Nat Comms. Nature Publishing Group*;
682 2018;9: 349. doi:10.1038/s41467-017-02789-2
- 683 59. Park S, Lee D-H, Park J-G, Lee YT, Chung J. A sensitive enzyme immunoassay for
684 measuring cotinine in passive smokers. *Clin Chim Acta*. 2010;411: 1238–1242.
685 doi:10.1016/j.cca.2010.04.027
- 686 60. Lee Y, Kim H, Chung J. An antibody reactive to the Gly63[ndash]Lys68 epitope of
687 NT-proBNP exhibits O-glycosylation-independent binding. *Experimental & Molecular*
688 *Medicine*. Nature Publishing Group; 2014;46: e114. doi:10.1038/emm.2014.57
- 689 61. Andris-Widhopf J, Steinberger P, Fuller R, RADER C, BARBAS CF III. Generation
690 of Human scFv Antibody Libraries: PCR Amplification and Assembly of Light- and
691 Heavy-Chain Coding Sequences. *Cold Spring Harbor Protocols*. Cold Spring Harbor
692 Laboratory Press; 2011;2011: pdb.prot065573–pdb.prot065573.
693 doi:10.1101/pdb.prot065573
- 694 62. BARBAS CF III, Burton DR, Scott JK, Silverman GJ. *Phage Display: A Laboratory*
695 *Manual*. Cold Spring Harbor Laboratory Press. 2001. doi:10.1086/420571
- 696 63. Lee S, Yoon I-H, Yoon A, Cook-Mills JM, Park C-G, Chung J. An antibody to the
697 sixth Ig-like domain of VCAM-1 inhibits leukocyte transendothelial migration without
698 affecting adhesion. *J Immunol. American Association of Immunologists*; 2012;189:
699 4592–4601. doi:10.4049/jimmunol.1103803
- 700 64. Kim H-Y, Tsai S, Lo S-C, Wear DJ, Izadjoo MJ. Production and Characterization of
701 Chimeric Monoclonal Antibodies against *Burkholderia pseudomallei* and *B. mallei*
702 Using the DHFR Expression System. Chakravorty D, editor. *PLoS ONE. Public*
703 *Library of Science*; 2011;6: e19867. doi:10.1371/journal.pone.0019867
- 704 65. REED LJ, MUENCH H. A SIMPLE METHOD OF ESTIMATING FIFTY PER
705 CENT ENDPOINTS. *Am J Epidemiol. Oxford University Press*; 1938;27: 493–497.
706 doi:10.1093/oxfordjournals.aje.a118408
- 707 66. Kang CK, Choi SJ, Koh J, Jeon YK, Kim KH, Chung J, et al. 18F-FDG PET and
708 histopathologic findings in a patient with severe fever with thrombocytopenia
709 syndrome. *Ticks and Tick-borne Diseases*. 2018;9: 972–975.
710 doi:10.1016/j.ttbdis.2018.03.030
- 711 67. DULBECCO R, VOGT M. Some problems of animal virology as studied by the
712 plaque technique. *Cold Spring Harb Symp Quant Biol*. 1953;18: 273–279.

713

714 **Figure legends**

715 **Fig 1. Ab10 has *in vitro* neutralizing activity against Severe Fever with** 716 **Thrombocytopenia Syndrome virus (SFTSV)**

717 To measure neutralizing efficacy, Ab10 scFv-Fc fusion protein was mixed with 100 TCID₅₀
718 of SFTSV (strain: Gangwon/Korea/2012) and added to Vero cells. After incubation for 1 h,
719 the cells were washed and cultured for 2 days. Then, the Gn glycoprotein produced in
720 infected Vero cells was detected in an immunofluorescence assay using anti-SFTSV Gn
721 glycoprotein antibody, with at least five technical replicates. The fluorescence signal intensity
722 of stained SFTSV Gn glycoprotein was used as a quantitative indicator for viral infection. **(A)**
723 The proportion of infected cells compared to non-treated cells was defined as relative cell
724 infection (%) and was plotted. Mab4-5 scFv-Fc fusion protein was also treated in a parallel
725 experiment. Error bars represent standard deviations (s.d.), asterisks indicate a statistically
726 significant difference as determined by a nonparametric Friedman test with a post hoc Dunn's
727 multiple comparison test (* $P \leq 0.05$, ** $P \leq 0.01$, *** $P \leq 0.001$, **** $P \leq 0.0001$). **(B)**
728 Representative images of each treatment group are shown (scale bar, 100 μm). SFTSV Gn
729 glycoprotein and nuclei were stained in FITC (green) and DAPI (blue), respectively.

730

731 **Fig 2. Ab10 protected mice from SFTSV infection**

732 The overall scheme for the administration of virus and antibody is described in **(A)**. Eight-
733 week-old A129 mice ($n = 5$ per group) were inoculated with 2 or 20 PFU of SFTSV through
734 a subcutaneous route. At 1, 24, 48, and 72 h post infection, infected mice were
735 intraperitoneally administered with 600 μg of Ab10, MAb4-5, IgG₁ isotype control antibody,
736 or PBS vehicle control. Percentages of survival **(B)** and body weight relative to the day of
737 virus inoculation **(C)** were monitored daily until 10 days post infection. Survival was

738 determined by the Kaplan-Meier method. Relative body weight values in (C) are presented as
739 the means with standard deviations of surviving mice in each group.

740

741 **Fig 3. Delayed administration of Ab10 also protected mice from SFTSV infection up to**
742 **3 days after inoculation of the virus**

743 The overall scheme for the virus challenge and delayed antibody administration are described
744 in (A). Eight-week-old A129 mice (n = 5 per group) were inoculated with 2 or 20 PFU of
745 SFTSV through a subcutaneous route. From 1, 3, 4, or 5 days post infection, infected mice
746 were intraperitoneally administered with 600 µg of Ab10 per day for 4 consecutive days.
747 Percentages of survival (B) and weight relative to the day of virus inoculation (C) were
748 monitored daily until 10 days post infection. Survival was determined by the Kaplan-Meier
749 method. The values in (C) are presented as the means with standard deviations of surviving
750 mice in each group.

751

752 **Fig 4. Ab10 also bound to Gn glycoprotein of HB29 and SD4 strains with comparable**
753 **affinity to that of Gangwon/Korea 2012.**

754 Binding properties of human IgG₁ monoclonal antibody Ab10 (A) and MA4-5 (B) to
755 recombinant Gn glycoprotein ectodomain of Gangwon/Korea 2012, HB29, and SD4 strains
756 were measured by enzyme-linked immunosorbent assay (ELISA). Non-linear regression
757 curves were fitted to a one site specific saturation binding model and the mean absorbance at
758 450 nm with standard deviation (s.d.) error bars are shown at each antibody concentration.
759 (C) Surface plasmon analysis of Ab10 antibody was performed on the CM5 chip with an
760 immobilized anti-histidine antibody binding to poly-histidine tagged SFTSV Gn ectodomain.
761 The experimental data at concentrations of 80, 40, 20, 10, 5, 2.5, and 1.25 nM Ab10 antibody

762 are shown in color, and the fitted curves are shown in black. Calculated rate constants are
763 shown in the table.

764

765 **Fig 5. The epitope of Ab10 was determined by alanine mutant analysis**

766 The conformational epitope of Ab10 antibody on Gn glycoprotein ectodomain was
767 determined by measuring antibody binding activity to recombinant mutant proteins with
768 amino acid residues that were substituted with alanine at residues corresponding to 315-389.
769 **(A)** Epitopes predicted by cross-linker assisted mass spectrometry are shown in red, and
770 alanine substituted residues that affected Ab10 antibody binding are shown in purple. The
771 overlapping domain II (blue annotation) and region upstream of the stem region (gray
772 annotation) are also indicated. **(B)** The reactivity of Ab10 to each alanine mutant is
773 represented as relative reactivity, which was calculated using absorbance values (Abs) as
774 follows: % Relative reactivity = $[100 \times \{(Abs \text{ of mutant captured by Ab10}) / (Abs \text{ of mutant}$
775 $\text{captured by HA antibody})\} / \{(Abs \text{ of wildtype captured by Ab10}) / (Abs \text{ of wildtype}$
776 $\text{captured by HA antibody})\}]$. Bars indicate the mean and standard deviation (s.d.).

777

778 **Supporting information**

779 **S1 Fig. Inhibition of cytopathic effect by SFTSV**

780 The cytopathic effects (CPE) of SFTSV on Vero cells were monitored to evaluate the
781 protective effect of antibody clones. Vero cells at 80% confluency grown in 96-well tissue
782 culture plates were exposed to 100 μ l of SFTSV-antibody mixture, which was prepared by
783 mixing 100 TCID₅₀/ml SFTSV (Strain: Gangwon/Korea/2012) and 100 μ g/ml candidate
784 antibody (scFv-Fc format) at the 1:1 volumetric ratio, and was then pre-incubated for 1 h.
785 After incubating the SFTSV-antibody mixture with cells for 1 h, cells were washed with PBS

786 followed by addition of fresh growth medium for 96 h. Cells were observed under a
787 microscope to evaluate CPE. In control groups, cells not incubated with virus (Uninfected),
788 cells infected without antibody treatment (Infected), cells incubated with virus, and the
789 isotype control antibody (Isotype control antibody) were employed.

790

791 **S2 Fig. Amino acid sequences of Ab10 antibody variable region**

792 The amino acid sequence of light chain variable region (**A**) and heavy chain variable region
793 (**B**) are shown. Blue letters indicate complementary determining regions (CDR) of each
794 variable region defined by the International Immunogenetics Information System (IMGT).

795

796 **S3 Fig. Focus forming assay using Ab10**

797 Thirty to 50 focus forming units (FFU) of SFTSV were incubated with Ab10 scFv-Fc fusion
798 protein at concentrations from 1.95 to 1,000 nM for 1 h at 37°C and added to Vero cells in a
799 24-well tissue culture plate. After incubation for 1 h at 37°C in a 5% CO₂ incubator, cells
800 were overlaid with 1% methylcellulose in culture medium RPMI with 2% FBS and cultured
801 for 2 days. For detection of SFTSV localized clusters (foci), cells were fixed with a 10%
802 formalin solution for 1 h and incubated with 5 µg/ml of anti-SFTSV Gn glycoprotein
803 detection antibody. After the washing step, cells were incubated for 1 h at room temperature
804 with 1:100 diluted fluorescein isothiocyanate (FITC)-conjugated anti-rabbit IgG Fc antibody
805 (111-095-046, Jackson ImmunoResearch). FFU were determined by counting visible foci
806 under an automated inverted fluorescence microscope (DMI4000 B, Leica). Neutralization
807 efficacy was calculated as the % decreased fraction in the number of foci compared to that of
808 the isotype antibody control group. Dose-response curves were drawn by non-linear

809 regression analysis and fitted to the EC90 (variable slope model). A Mab4-5 scFv-Fc fusion
810 protein was used as a positive control.

811

812 **S4 Fig. Phylogenetic analysis of SFTSV Gn glycoprotein ectodomain**

813 The amino acid sequence of Gn glycoprotein from 272 SFTSV isolates deposited in ViPR
814 were used for analysis. The sequences were trimmed to retain the amino acid residues from
815 20–452 that corresponded to the ectodomain. Trimmed sequences were analyzed, and a
816 phylogenetic tree was built in a circular tree layout using the neighbor-joining method with a
817 Jukes-Cantor genetic distance model. The names of isolates are labeled beside the tip of each
818 branch. Asterisks at the tip of branches indicate the isolates that were tested for binding
819 activity of Ab10.

820

821 **S5 Fig. Immunoblot of recombinant Gn-Cκ fusion protein using anti-Gn antibodies**

822 Recombinant SFTSV Gn-Cκ was prepared with sample buffer and reducing agent (NP0008
823 and NP0004, Invitrogen). The samples were then separated on a polyacrylamide gel
824 (NP0321BOX, Invitrogen) by electrophoresis and transferred to a nitrocellulose membrane.
825 After blocking with 5% (w/v) skim milk in Tris-buffered saline (pH 7.4) the membrane was
826 incubated with 100 ng/ml of five (Ab6 to Ab10) SFTSV Gn specific antibodies in a scFv-Fc
827 format. Gn bound antibodies were probed with HRP-conjugated anti-human IgG Fc antibody
828 (31423, Invitrogen). To confirm the presence of Gn-Cκ protein, HRP-conjugated anti-human
829 Ig kappa light chain antibody (AP502P, Chemicon) was used to directly detect Gn-Cκ. The
830 blots were visualized using a chemiluminescent substrate (34578, Thermo Scientific).

831

832 **S6 Fig. Phylogenetic analysis of sequences covering Ab10 epitope**

833 The amino acid sequence of Gn glycoprotein from the 272 SFTSV isolates deposited in ViPR
834 were analyzed. The sequences were trimmed to retain the amino acids from 313–389 that
835 correspond to the residues recognized by Ab10. Trimmed sequences were analyzed and a
836 phylogenetic tree was built in a circular tree layout using the neighbor-joining method with a
837 Jukes-Cantor genetic distance model. The names of isolates are written beside the tip of each
838 branch. Strain names labeled in red indicate that the Gn glycoprotein of the indicated strain is
839 predicted to not interact with Ab10.
840

841

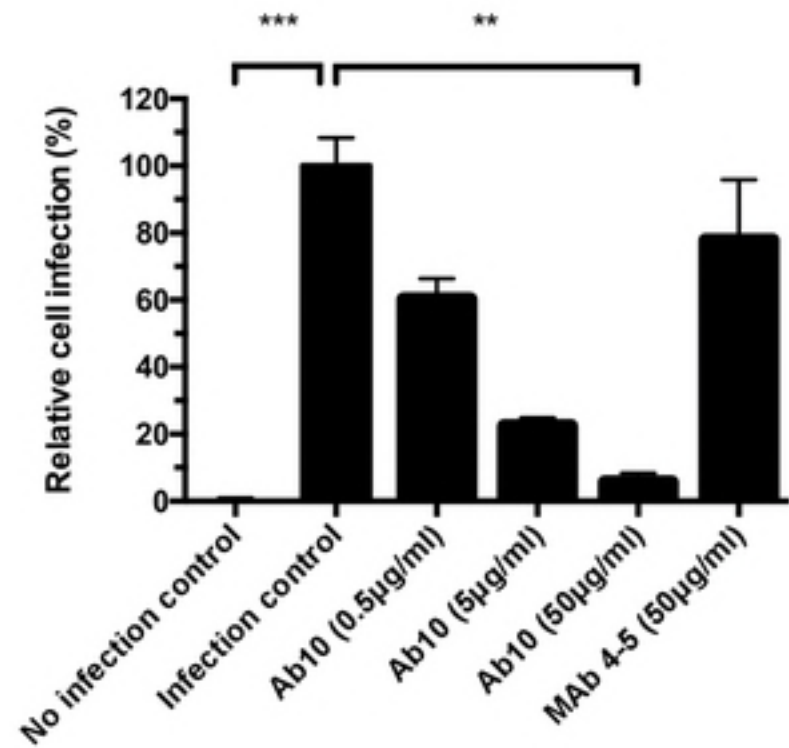
842 **Data availability**

843 All relevant data are contained within the paper and its Supporting Information files.

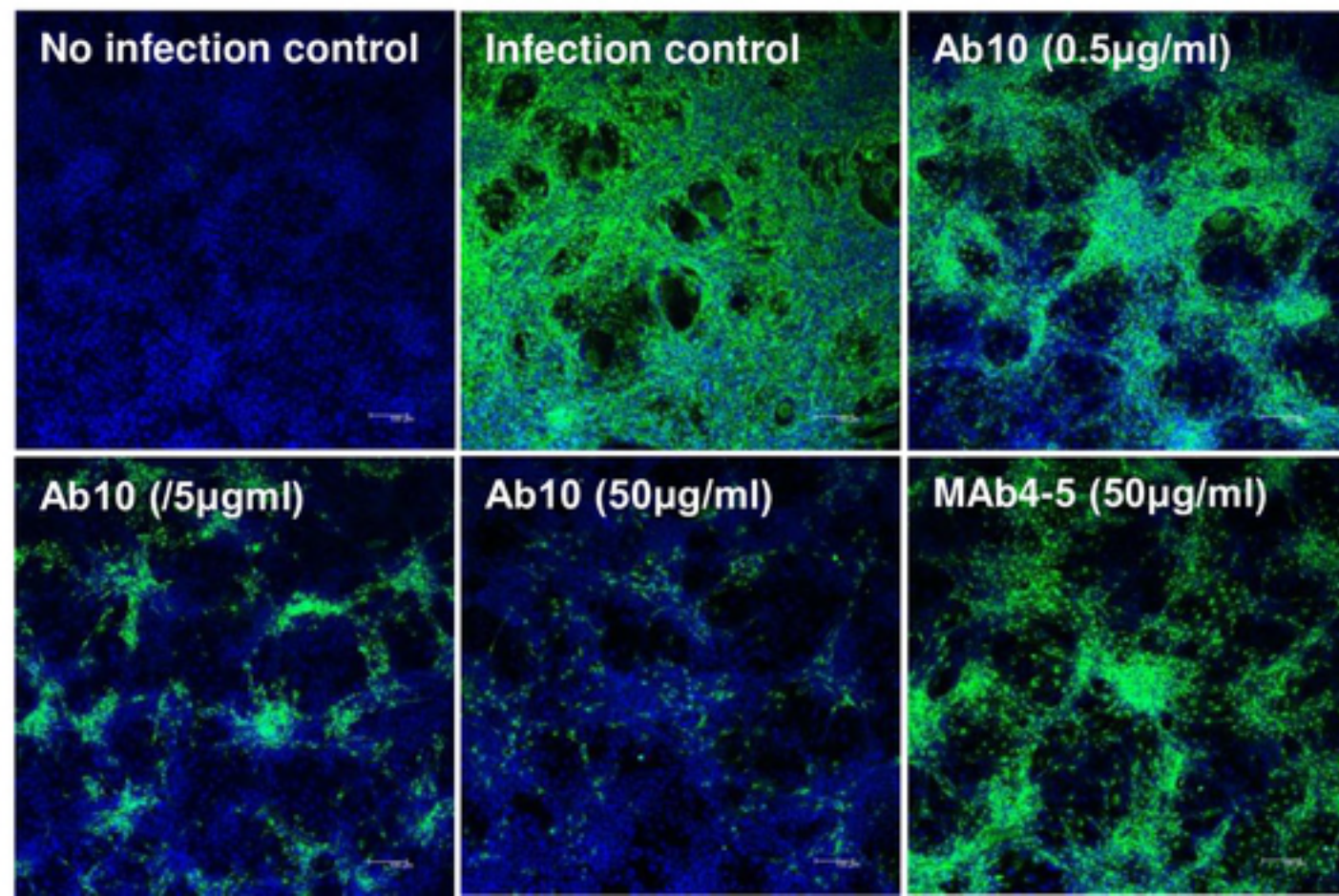
844

845

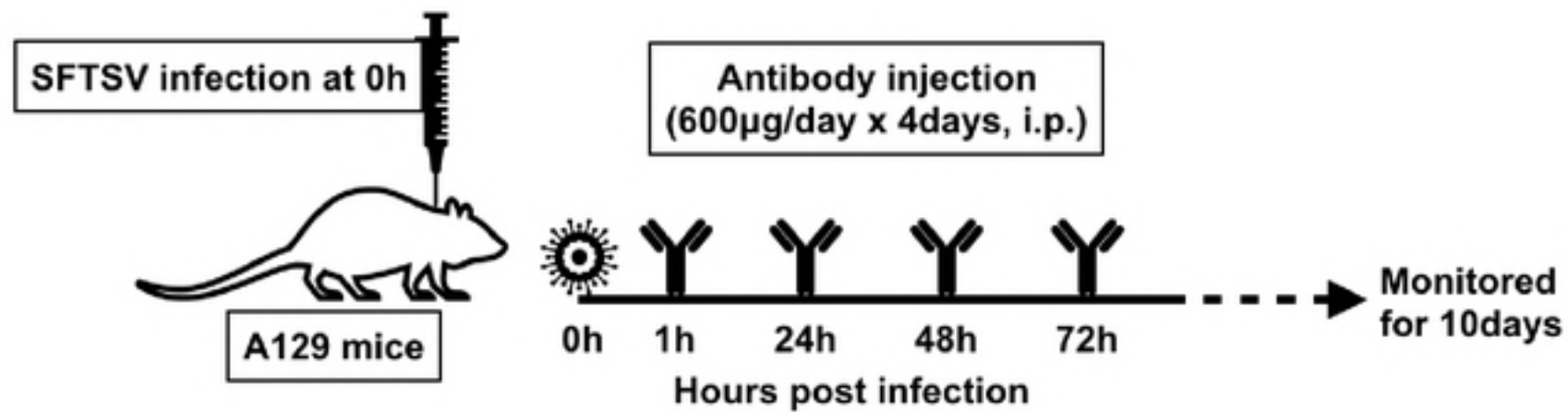
A



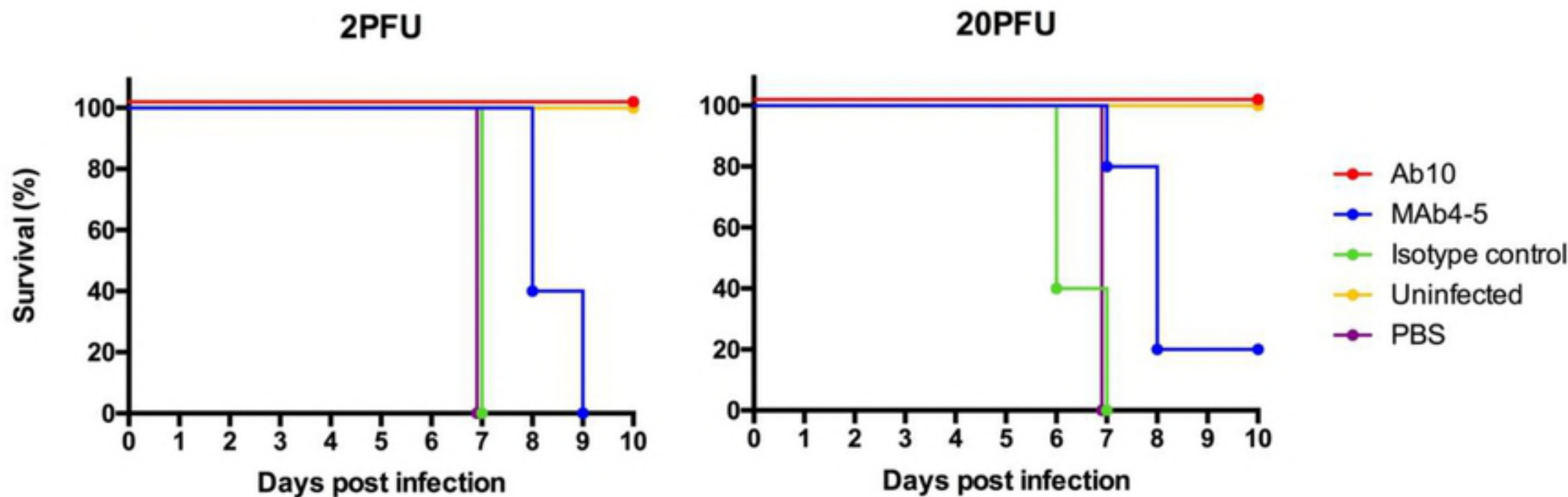
B



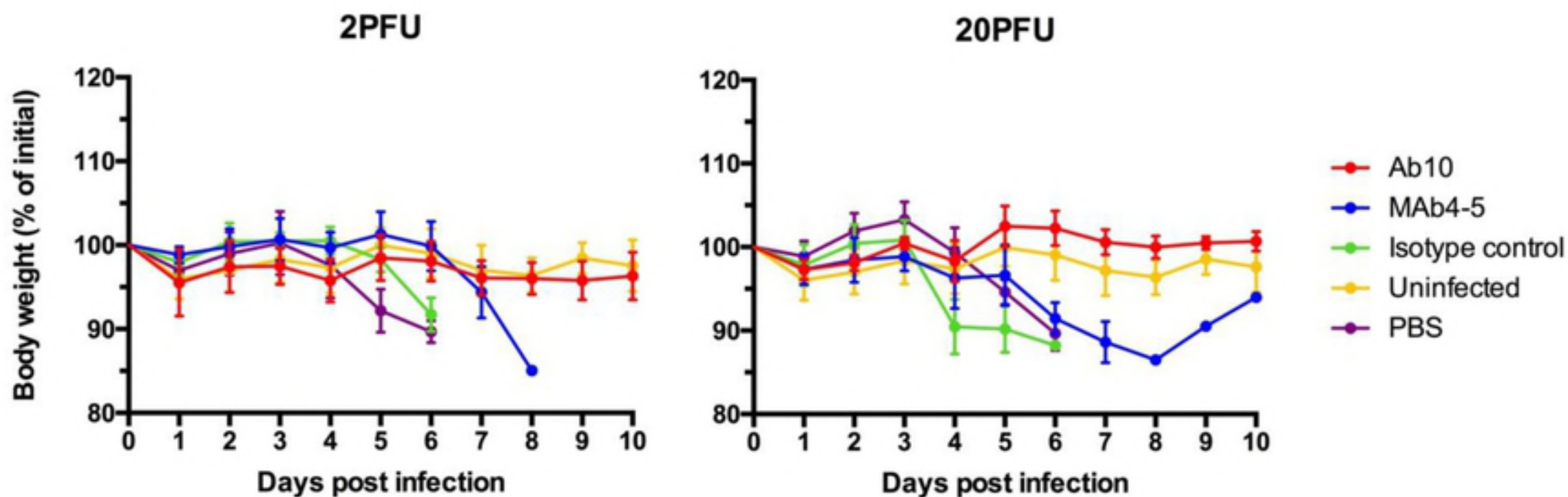
A



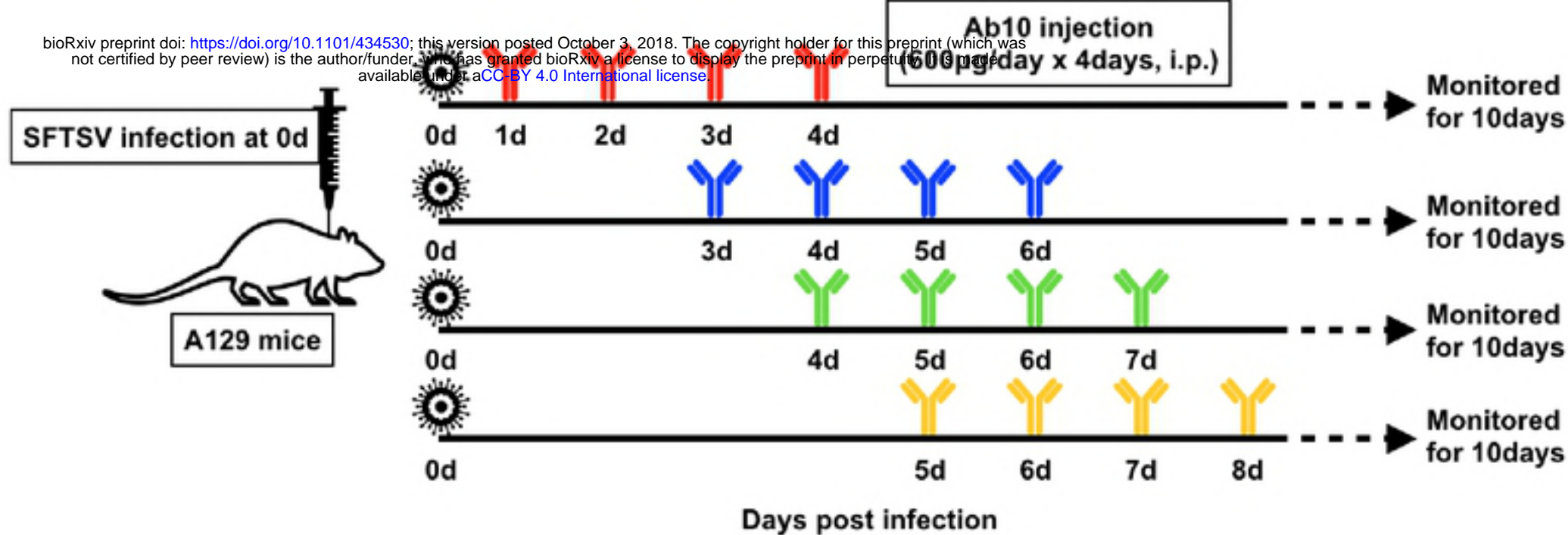
B



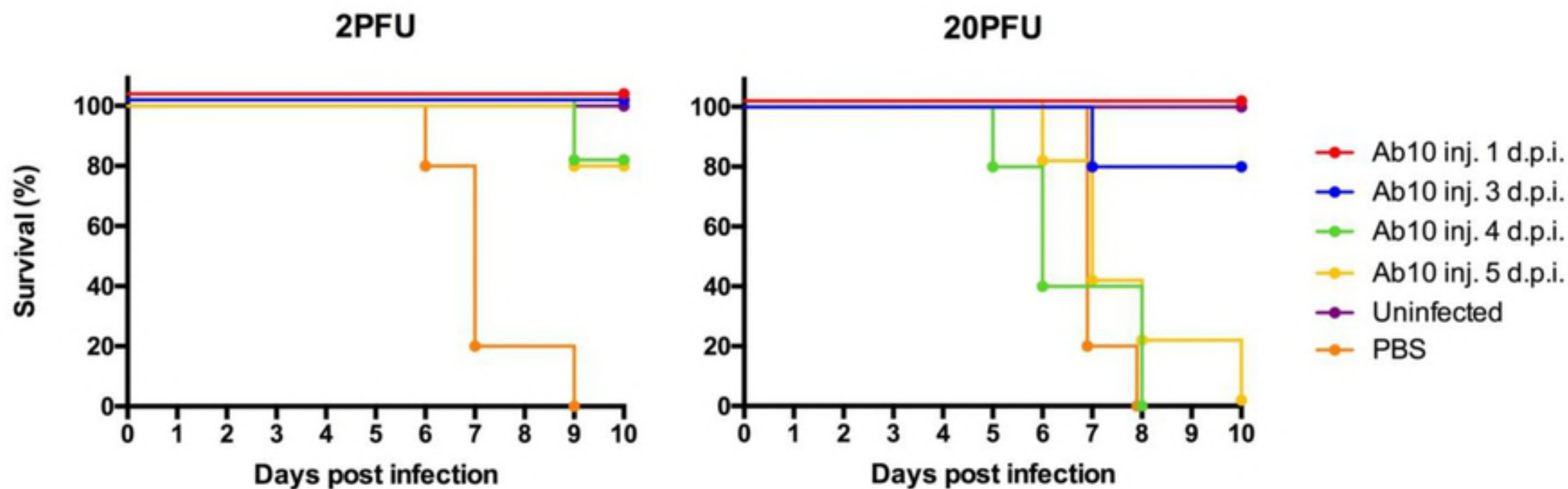
C



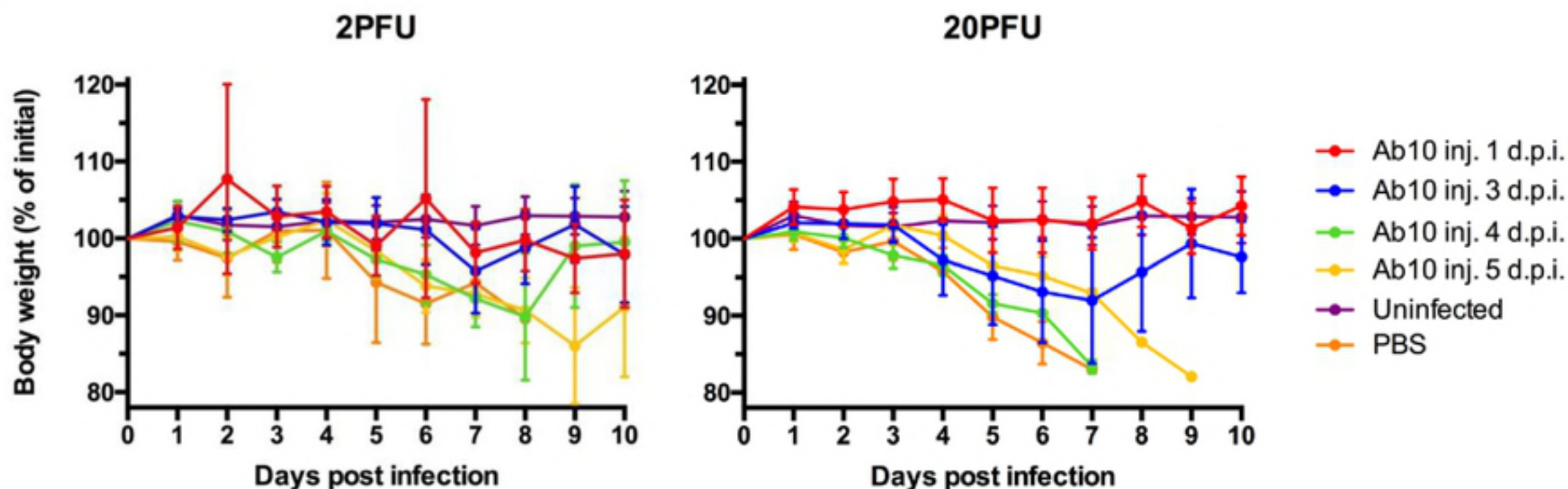
A

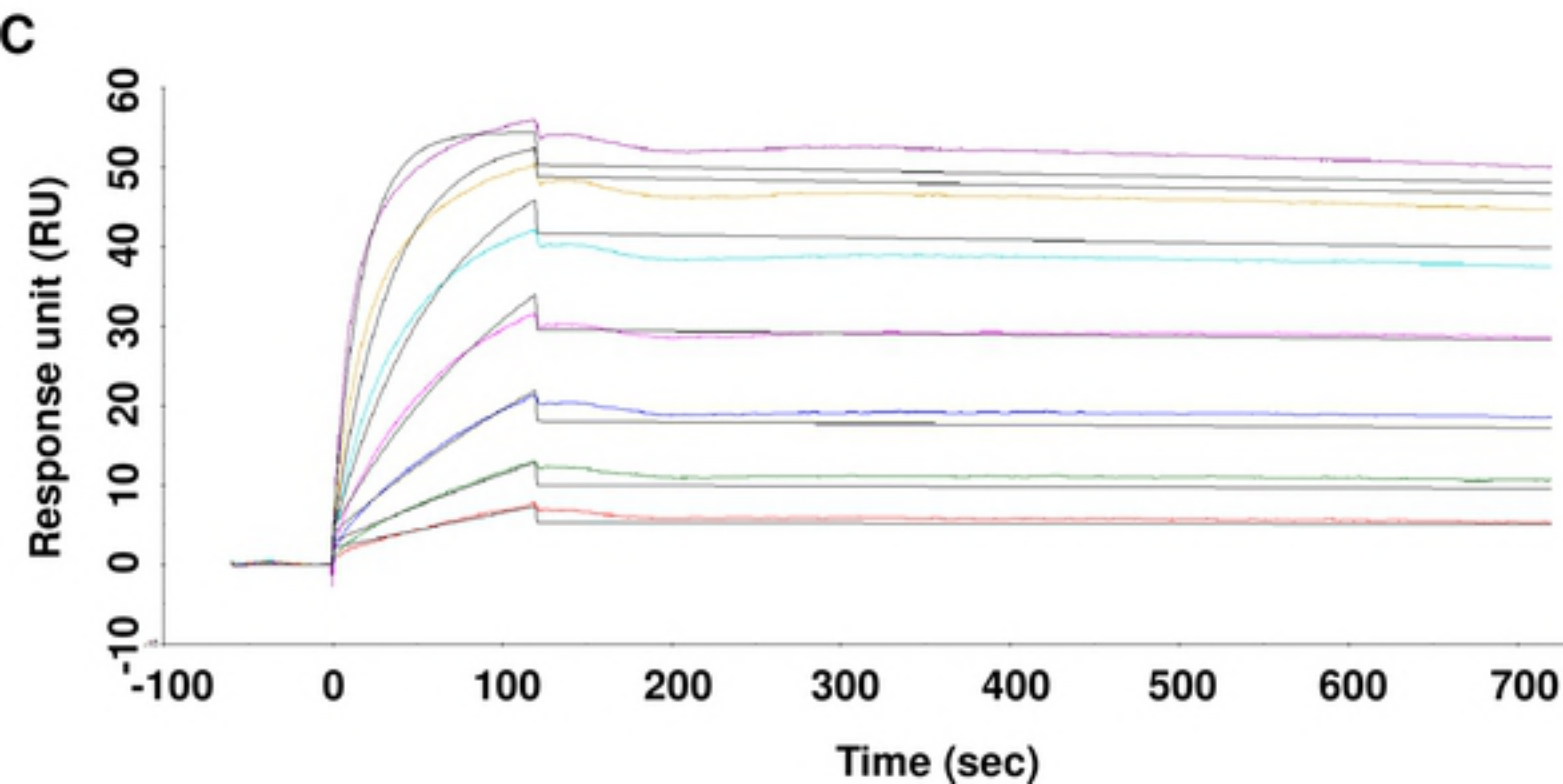
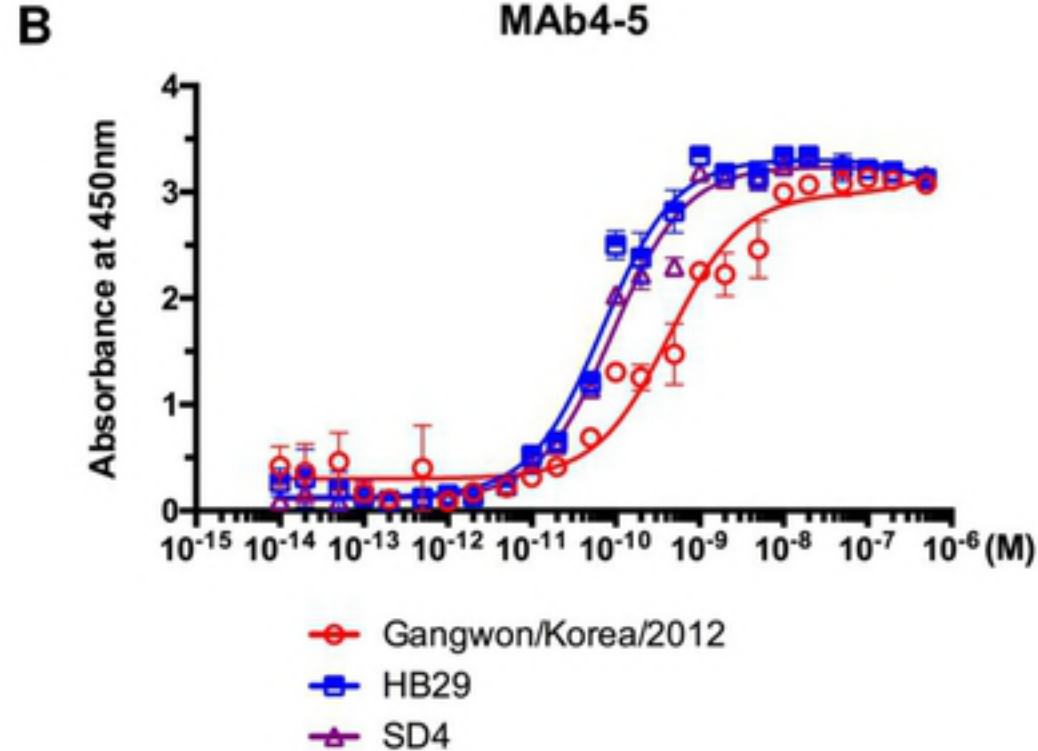
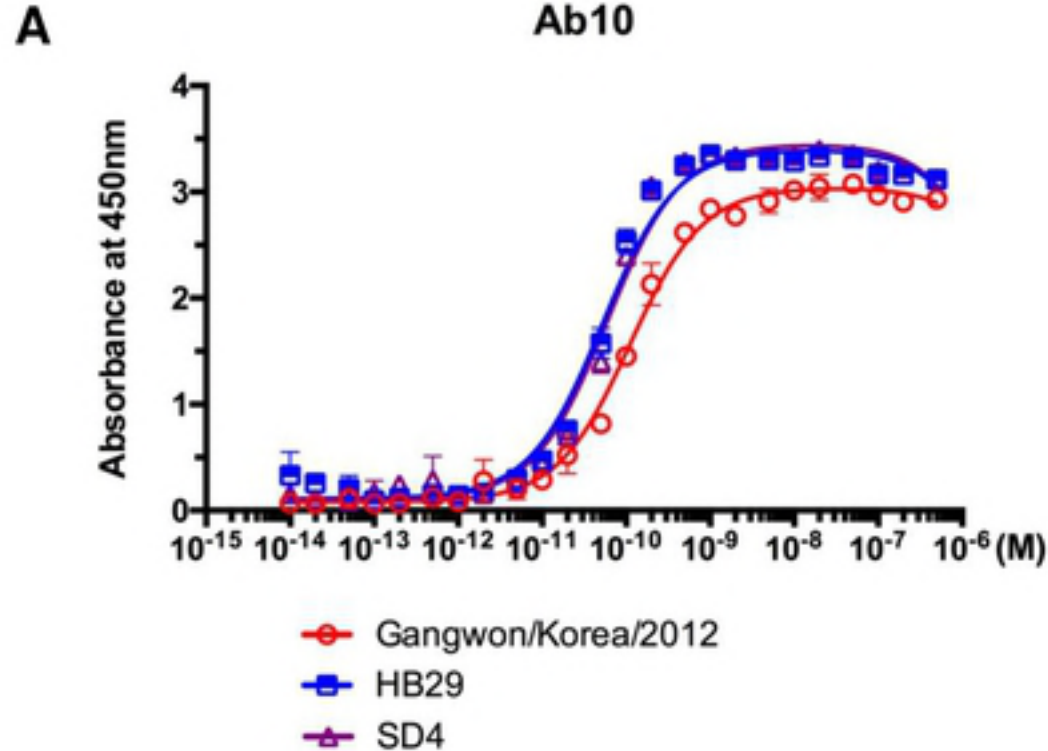


B

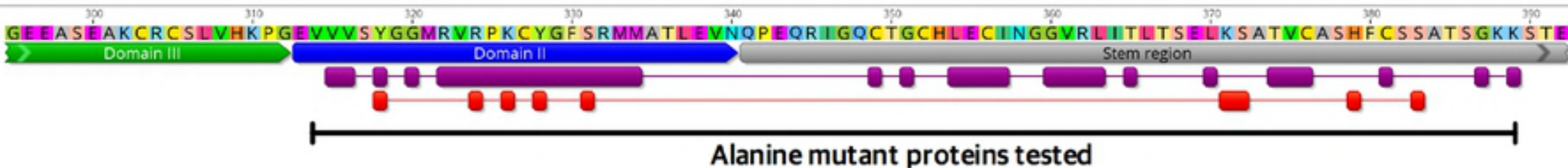
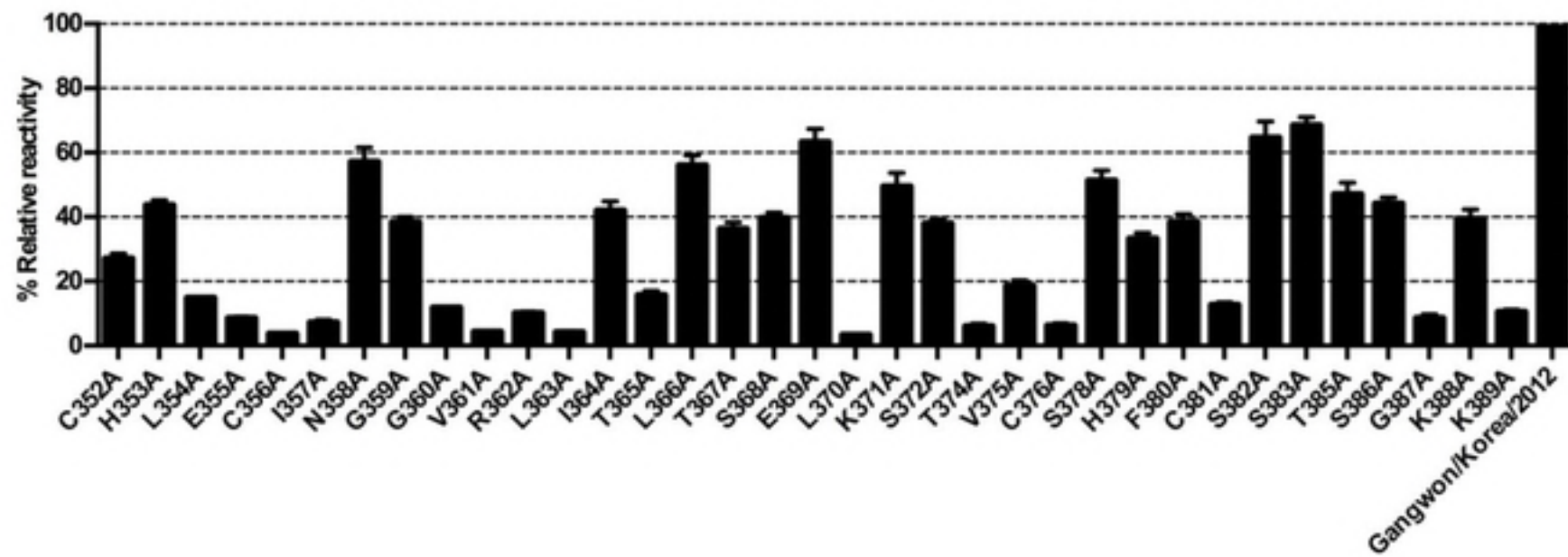
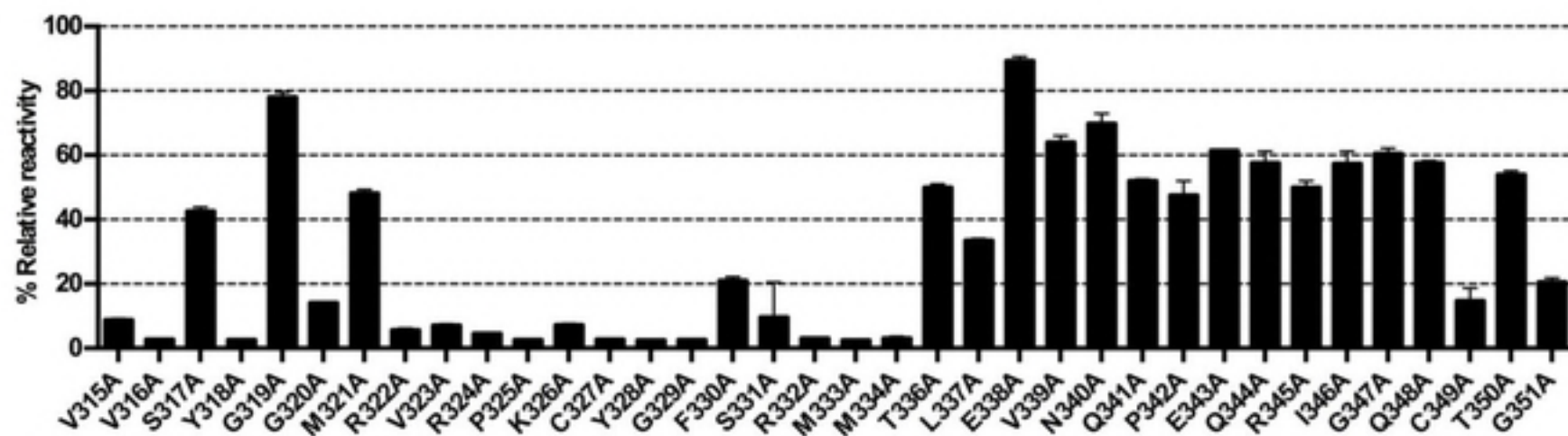


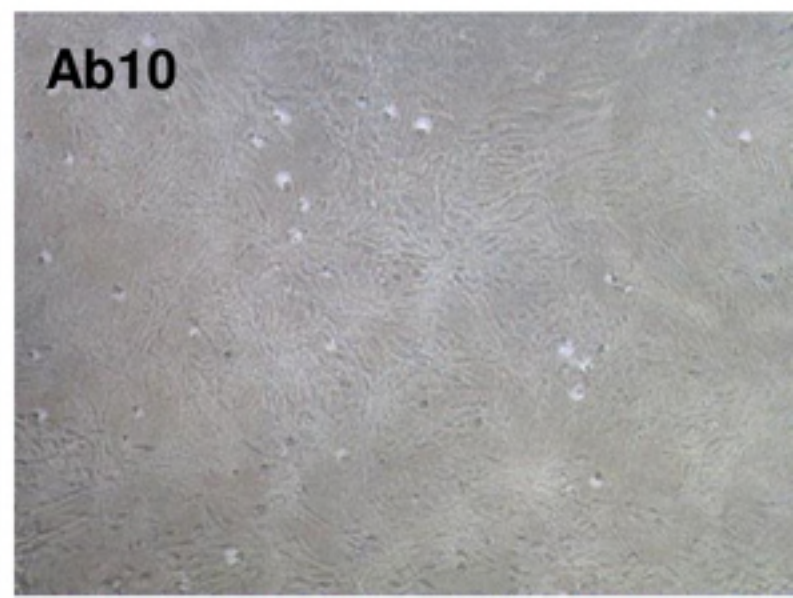
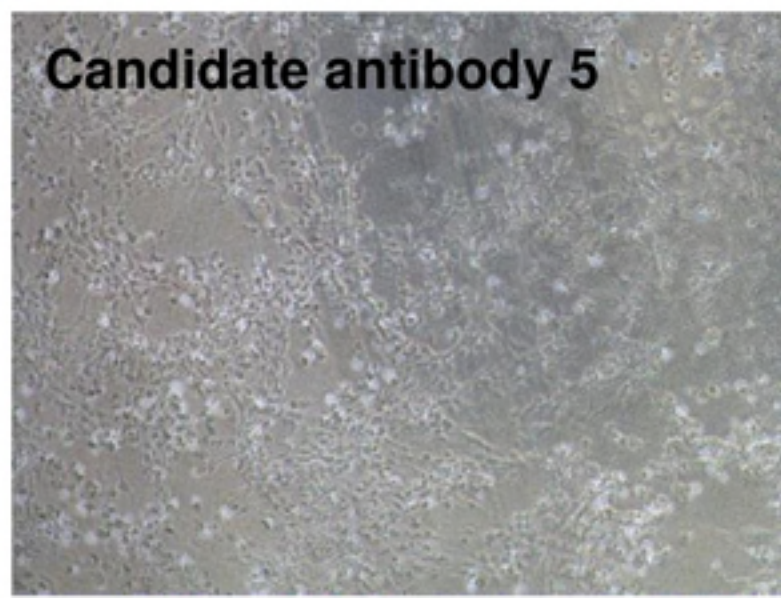
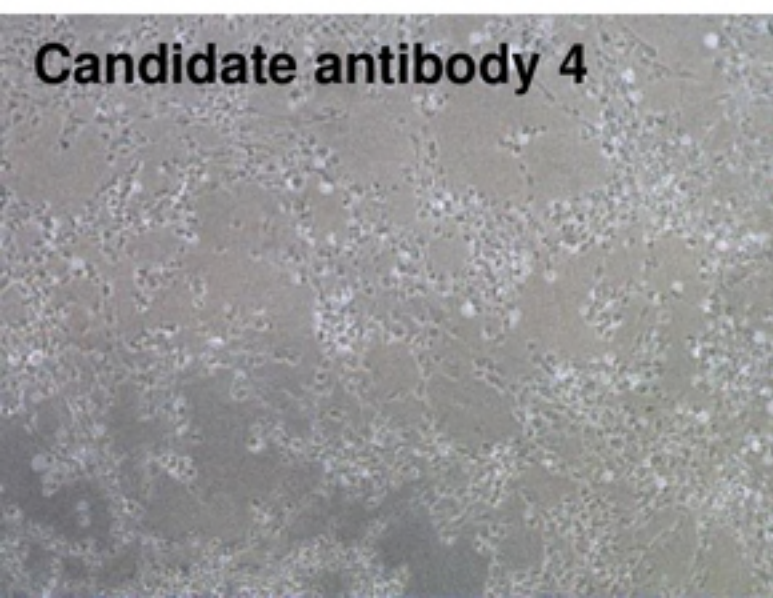
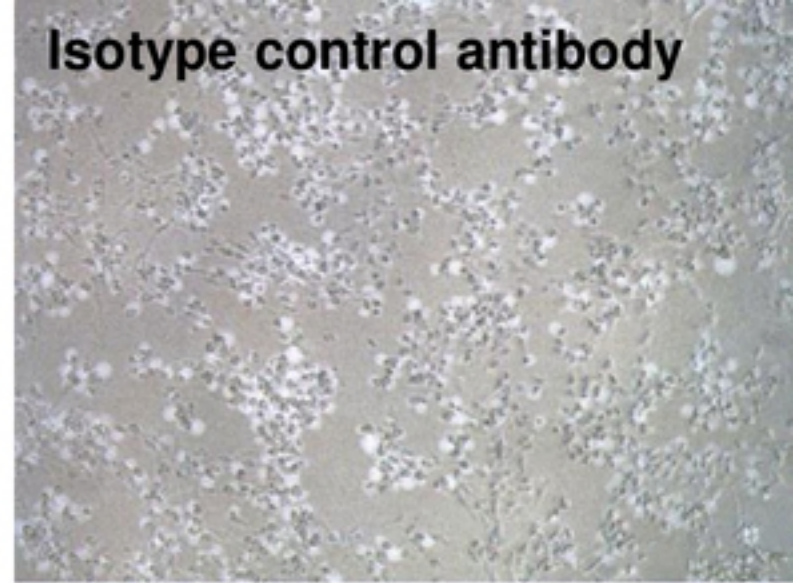
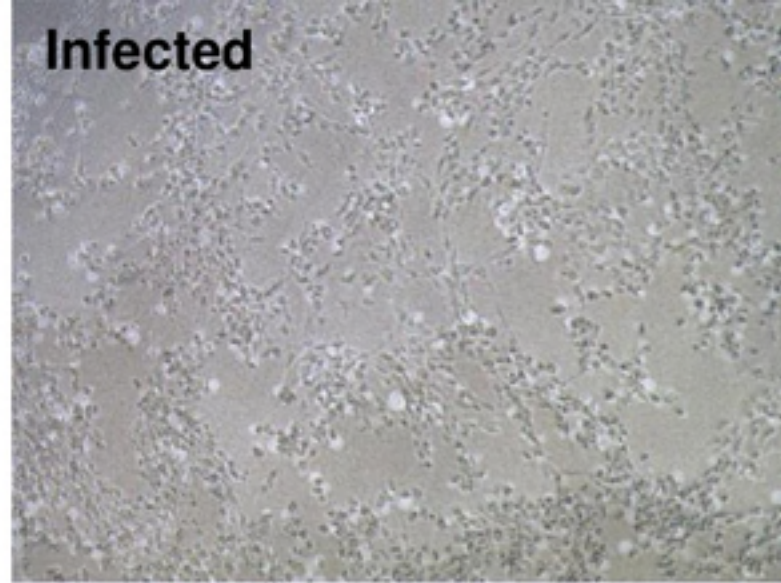
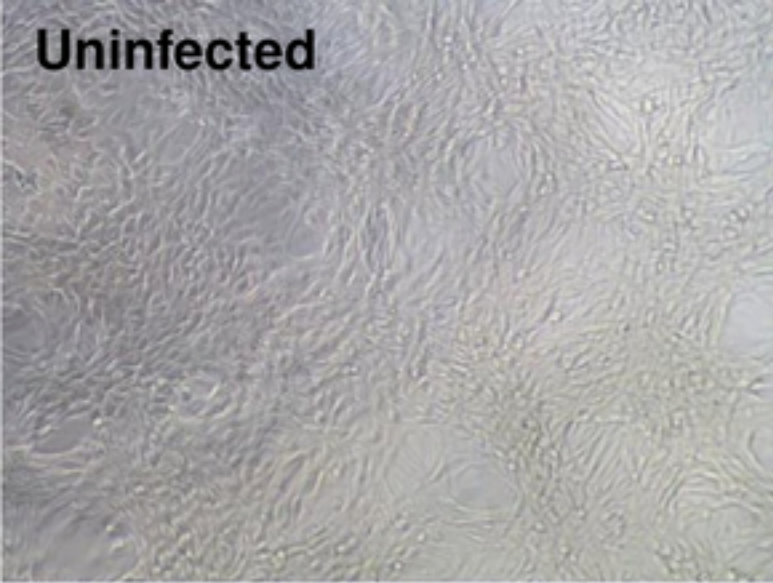
C





Association rate K_{on} [M ⁻¹ s ⁻¹]	7.4×10^5
Dissociation rate K_{off} [s ⁻¹]	7.7×10^{-5}
Affinity K_D [M]	1.0×10^{-10}

A**B**

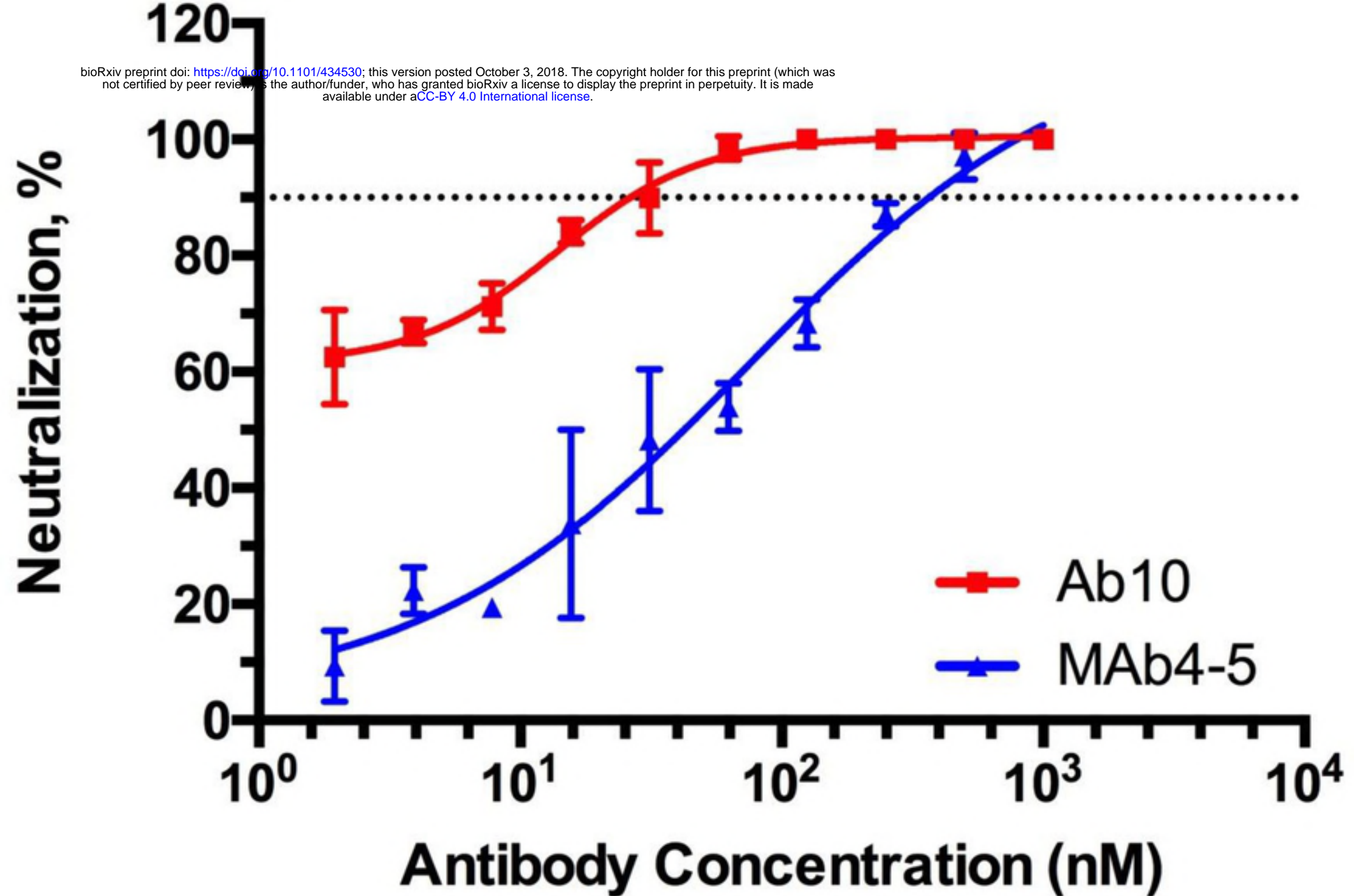


A

1 10 20 30 40 50 60 70 80 90 100
E L V M T Q S P S S L S A S V G D T V T I T C R A S Q S I Y T Y L N W Y H Q T P G K A P K L L I S A A S S L Q S G V P S R F S G S G S G T D F T L T I S S L Q P E D F A T Y Y C Q Q Y A D V P V T F G G
G T K L E I K¹⁰⁷

B

1 10 20 30 40 50 60 70 80 90 100
E V Q L V E S G G G V V Q P G R S L R L S C A A S G F T F S G Y G I H W V R Q A P G K G L E W V A L I S Y D G S N K Y Y A D S V K G R F T I S R D N S K N T L Y L Q M N S L R A E D T A V Y Y C A K D R
D Y F G S G F D Y W G Q G T L V T V S S^{110 121}



EC_{90} for Ab10: 55.6 nM

(30.89 to 100.1, 95% Confidence Intervals)

EC_{90} for MAb4-5: 1.8 μ M

(95.92 to 34755, 95% Confidence Intervals)

bioRxiv preprint doi: <https://doi.org/10.1101/434530>; this version posted October 3, 2018. The copyright holder for this preprint (which was not certified by peer review) is the author/funder, who has granted bioRxiv a license to display the preprint in perpetuity. It is made available under aCC-BY 4.0 International license.



Gn-Cx

Ab6

Ab7

Ab8

Ab9

Ab10

97.4kDa

69kDa

55kDa

